Accepted Manuscript

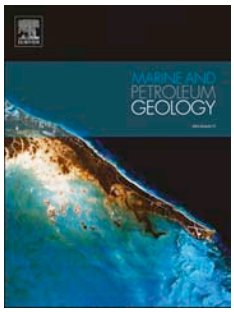

Submarine slide blocks and associated soft-sediment deformation in deep-water basins: A review

Tiago M. Alves

PII: S0264-8172(15)00159-2

DOI: 10.1016/j.marpetgeo.2015.05.010

Reference: JMPG 2238

To appear in: *Marine and Petroleum Geology*

Received Date: 22 July 2014

Revised Date: 5 May 2015

Accepted Date: 11 May 2015

Please cite this article as: Alves, T.M., Submarine slide blocks and associated soft-sediment deformation in deep-water basins: A review, *Marine and Petroleum Geology* (2015), doi: 10.1016/j.marpetgeo.2015.05.010.

Submarine slide blocks and associated soft-sediment deformation in deep-water basins: A review

Tiago M. Alves[1]

1) 3D Seismic Lab – School of Earth and Ocean Sciences, Cardiff University – Main Building, Park Place, Cardiff, CF10 3AT, United Kingdom (alvest@cardiff.ac.uk)

ABSTRACT

Three-dimensional (3D) seismic and outcrop data are used to review the significance of submarine slide blocks and associated soft-sediment deformation structures in deep-water basins. Submarine slide blocks are generated during major instability events in a variety of geological settings and their size exceeds that of boulders, which are <4.1 m. Slide blocks can be ~500 m high by >4.5 km long on a number of continental margins, presenting internal folding, thrusting and rolling over basal breccia-conglomerate carpets. In addition, soft-sediment deformation structures such as foliated strata, intrafolial folds, tiling, bookshelf sliding and dilational jogs reflect important shearing within blocks and their basal glide planes. This work proposes that buried blocks and associated coarse-grained debrites are capable of forming prolific reservoir intervals for hydrocarbons and mineralization. Three-dimensional leakage factor models show the bulk of fluid flow to be focused in vertical and horizontal surfaces within, and immediately below displaced blocks. The generation of large slide blocks can also mark the sudden release of overburden pressure above existing hydrocarbon fields, and resulting loss of seal competence. Ultimately, this review clarifies the present-day understanding on the modes of formation of submarine slide blocks, confirming their economic importance in deep-water basins throughout the world.

Keywords: Deep-water basins; submarine slides; blocks; structure; kinematic indicators; hydrocarbons.

1. Introduction

Stratigraphic intervals containing large slide blocks are common in deep-water basins, being a consequence of major slope instability events (Kvalstad et al., 2005; Jenner et al., 2007, Deptuck et al., 2007). Slide blocks comprise relatively undeformed strata of metre to kilometre scales preserved within a fine-grained matrix with diverse lithologies, including coarse-grained sands, conglomerates and breccias (e.g. Duffield et al., 1982; Moore et al., 1995; Talling et al., 2007). As a result, stratigraphic units containing slide blocks can form prolific hydrocarbon reservoirs such as those in the Eocene of South Texas, USA (Ogiesoba and Hammes, 2012), in the Gulf of Mexico (Edwards, 2000) or offshore Nigeria (Clayton et al., 1998; Apotria et al., 2004; Bruso et al., 2004). When buried at lower-crust depths, slide blocks can also contain important mineralization, particularly when forming different strata from the matrix rock in which they are included (Wendorff, 2000; 2005; 2011).

In this work, the terms ‘submarine slide block’, or ‘block’ as used herein, refer to large volumes of undeformed to moderately deformed strata generated in submarine environments and transported by mass-wasting processes (Borgomano, 2000; Emmerich et al., 2005; Kvalstadt et al., 2005; Spence and Tucker, 1997). Most blocks slide over a well defined shear plane that is irregular or indented (Hampton, 1972; Embley, 1980; Hühnerbach and Masson, 2004; Masson et al., 2006; Moscardelli et al., 2006). Over these basal shear planes, transporting distances of more than 100 km are effectively recorded by outrunner blocks, particularly on the flanks of active volcanoes (Masson, 1996; Masson et al., 2002) and tectonically active slopes (Roep and Fortuin, 1996; De Blasio et al., 2006).

Blocks can have a sedimentary or a tectonic origin, and are often included in sets of strata specifically generated in submarine instability events, called Mass-Transport Deposits (MTDs) or Complexes (MTCs) on seismic data, or olistostromes at outcrop. As shown in this paper, the internal structure and size of blocks reflect distinct downslope transporting styles, which include

rotational sliding, gliding, block drag, skipping, toppling, free fall, and translation over high-density flows. Important soft-sediment deformation is recorded at the base of displaced blocks.

Individual blocks recognised on seismic, sidescan sonar or bathymetric data are usually >5-10 m long, with the largest features approaching 500 m in height by >4.5 km in length (Alves et al., 2010; Dunlap et al., 2010; 2013; Alfaro and Holz, 2014; Gamboa and Alves, 2015a; Principaud et al., 2015). Blocks, or *megaclasts* as defined by Blair and MacPherson (1999), are by definition larger than boulders (>4.1 m) and show characteristic features in deep-marine settings around the world. These features are:

a) Blocks are commonly associated with slope instability events triggered by major tectonic phases, most of which relate to important uplift, exhumation and erosion of the upper crust (Roep and Fortuin, 1996; Dunlap et al., 2013).

b) Large fields of blocks accompany the transport of significant volumes of sediment into sedimentary basins (Drzewiecki and Simó, 2002; Di Francesco et al., 2010; Perotti et al., 2012).

c) Blocks comprise allochthonous strata displaced over significant distances, and can include successions uncharacteristic of the basins in which they accumulate (Bosellini et al., 1993, Odonné et al., 2011).

This paper reviews the significance of submarine slide blocks in geological and economic terms, at a time when deep-water stratigraphic successions reveal their presence throughout the world, from East Canada to the South Atlantic, Australia and Gulf of Mexico. After the methodology section, this work presents a summary of published case-studies in the geological record. Later, three-dimensional (3D) seismic data from SE Brazil and SE Japan are interpreted to describe diagnostic features of submarine slide blocks (Figs. 1 and 2). New data from two of the best exposed Miocene palaeoslopes in Europe, the Ierapetra Basin in SE Crete and the Tabernas-Sorbas Basin in SE Spain, are used to describe soft-sediment kinematic indicators at outcrop (metre) and

borehole (centimetre) scales (Figs. 1 and 3). An attempt has been made to clearly distinguish soft-sediment deformation structures from later tectonic structures (e.g., Postma et al., 1994). The remobilisation and deformation styles of blocks at sub-seismic scales are also described. The discussion will be centred on four key research questions:

1) What pre-conditioning factors contribute to the generation of submarine slide blocks?

2) What structural and geotechnical parameters control block displacement on continental slopes?

3) What are the key structural and kinematic markers of block movement at seismic and outcrop scales?

4) What structures recognised in individual blocks control post-depositional fluid flow and seal unit competence?

2. Methodology

This work uses three-dimensional (3D) seismic data from the upper continental slope of Espírito Santo (SE Brazil) and the accretionary wedge of SE Japan (Nankai Trough), the latter of which was chosen to illustrate glide plane geometries (Figs. 1 and 2). Outcrop data from two Late Miocene paleoslopes in SE Crete and SE Spain are used as analogues for the structures observed on seismic data (Fig. 1).

The seismic volume interpreted in SE Brazil has a bin spacing of 12.5 m, a 2 ms vertical sampling window, and was acquired with a 6 x 5,700 m array of streamers. Data processing included resampling, spherical divergence corrections and zero-phase conversions undertaken prior to stacking, 3D pre-stack time migration using the Stolt algorithm and one-pass 3D migration. Published borehole data from Deep Sea Drilling Program (DSDP) Sites 356 (Kumar et al., 1977) and 515/516 (Barker, 1983; Barker et al., 1983; Gambôa et al., 1983), as well as the works of Bruhn

and Walker (1997), Chang et al. (1992), Meisling et al. (2001), Viana et al. (2003), Fiduk et al. (2004) and França et al. (2007), were used to identify and date seismic-stratigraphic units with submarine slide blocks. Based on the dominant frequency of the interpreted seismic volume (40 Hz), vertical seismic resolution varies between 12 and 19 metres in block-laden strata.

In SE Japan, a 3D volume in water depths ranging from 1750 m to 3200 m was used (Figs. 1 and 2b). The interpreted volume has an inline spacing of 12.5 m, for a crossline spacing of 18.75 m, and was acquired with a 2-source array with four receiver cables spaced 150 m apart. A 4500 m long receiver cable with 360 receiver groups at 12.5 m spacing was used during data aquisition, and produced nominal 60-fold data. Data processing included pre-stack multiple removal and data conditioning (e.g., amplitude recovery, time-variant filtering, and predictive deconvolution) followed by 3D pre-stack depth migration (Moore et al., 2009). Seismic resolution approaches 6 m at the depth range of erosional features interpreted in this paper, based on the dominant wavelength of ~24 m observed on synthetic logs and seismic profiles.

2.1 Seismic interpretation

In order to describe their morphology, the base and tops of blocks and adjacent MTDs were first interpreted to extract a series of seismic attribute maps. Seismic attributes of interest include root-mean-square (RMS) amplitude and coherence slices, which were used to visualise the geometry of remnant and rafted blocks. RMS amplitude maps depict average squared amplitude values from individual samples within a defined interval (Brown, 2004). Coherence attributes convert a seismic volume of continuity (normal reflections) into a volume of discontinuity to emphasise faults and stratigraphic limits (Brown, 2004). Block height was measured directly on vertical seismic profiles after converting these for true depths using borehole information in Barker et al. (1983) and França et al. (2007). Remnant and rafted blocks were interpreted based on the identification of kinematic indicators described in this work.

2.2. Outcrop data

Data from the Ierapetra Basin in SE Crete are used to illustrate key structural aspects of blocks (Figs. 3a and 3b). Geological maps from the basin have been published by Fortuin (1977), Postma and Drinia (1993), Postma et al. (1993), Ten Veen and Postma (1999a; 1999b) and Alves and Lourenço (2010). This paper builds on the work from Alves and Lourenço (2010) to provide a more detailed image of slope instability in SE Crete, and a reassessment of structural deformation as investigated in 2011 and 2013 (Fig. 3b and 3c).

2.3 3D Stress® modelling

3D Stress® was the primary tool used to assess fluid leakage across blocks in SE Brazil (Morris et al., 1996). The software was also used to model the behaviour of faults and chasms to changing vertical (overburden) loading in a blocky MTD in the Espírito Santo Basin (Fig. 1). In particular, dilation tendency and leakage factor can be modelled to assess the likelihood of a fault to dilate and transmit fluid based on pre-defined stress conditions.

Dilation tendency represents the difference between the normal stress on the fault (σ_n) and the minimum principal stress (σ_3), normalized with respect to the differential stress. Pore fluid pressure within the fault plane acts against the vertical stress causing dilation within the fault. With 3D Stress®, dilation tendency is calculated from the following equation (Morris et al., 1996):

$$\text{Dilation tendency} = (\sigma_n - \sigma_3)/ (\sigma_1 - \sigma_3) \qquad (1)$$

Similar to dilation tendency, leakage factor takes into account detailed information on fluid pressure and tensile strength of fault-zone or fracture-filling material, providing an indicator on the

fluid transmissivity of faults, chasms and strata. This parameter is used to quantify the transmissivity of faults and surfaces interpreted from seismic or GIS packages, providing information of their potential as a fluid conduit. Leakage factor is dimensionless and is defined as:

$$\text{Leakage factor} = P_f / (\sigma_n - \tau) \qquad (2)$$

with P_f and τ comprising pore fluid pressure and tensile strength of fault-zone or fracture-filling material (Morris et al., 1996).

This paper modelled the release in loading stresses at the seafloor that results from the generation of a blocky MTD from SE Brazil (Fig. 2a). Blocks are up to 400-m high in the interpreted area. Leakage factor was modelled across the largest of the blocks for average pore pressures of <10 MPa, i.e. for a pore pressure approaching that of a shallow reservoir as the Golfinho Field, located just below the interpreted blocks. The top of the blocks was considered to be the paleo-seafloor at the time of slope collapse. In a second phase, leakage factors where calculated for different burial depths in order to document the importance of faults, fractures and chasms on fluid flow well after block collapse. A value of 25 MPa per kilometre was considered in σ_1 calculations, whilst σ_2 and σ_3 were calculated using Eaton (1969) postulate that, for hydrostatic conditions:

$$\sigma_{hmin} = 0.25/0.75\ \sigma_v = 0.33\ \sigma_v \qquad (3)$$

An averaged value of $\sigma_2 = (\sigma_1 - \sigma_3)/2$ was assumed in the leakage factor calculations.

3. Geological setting

In the published literature, terms such as ‘megablocks’, olistostromes, olistoliths, rafts and slide blocks are often used as synonyms of submarine slide blocks. The term ‘megablock’ was originally

used for large blocks of rock collapsed over volcanic domes and seamounts (Siebert, 1984; Moore et al., 1995; Lipman et al., 2003; Famin and Michon, 2010). However, its meaning has often been extended to include large blocks transported *en masse* during slope instability events, regardless of the geological setting in which they occur (e.g. Principaud et al., 2015). Thus, 'megablock' and 'submarine slide blocks' are synonyms in the most recent literature.

The term olistostrome is chiefly used at outcrop to map scale when dealing with chaotic volumes of rock containing blocks that are older than the sediment units in which they are included (Faure and Ishida, 1990; Diaz-del-Rio et al., 2003; Shu et al., 2011). However, olistostromes can also be called sedimentary mélanges by some authors (e.g. Cowan, 1985; Cloos and Shreve, 1988a; 1988b; Matsuda and Ogawa, 1993) to include blocks translated by gravitational processes that are synchronous to enveloping strata. This latter character stresses the fact that mélanges do not necessarily need to be tectonic in origin, thus partly overlapping with submarine slide blocks in terms of their definition (A. Fagereng, pers. comm.).

Large blocks such as megaboudins and rafts can also relate to tectonic and gravitational phenomena. However, their genesis differs from the blocks considered in this work. Megaboudins are crustal-size tectonic blocks that were fragmented and displaced over ductile lithospheric material on hyperextended or convergent continental margins (Fossen, 2010; Sen et al., 2013). Tectonic rafts comprise large volumes of strata fragmented and displaced over a ductile shear zone, usually comprising salt or shale (Alves, 2012; Quirk et al., 2012; Pilcher et al., 2014). Rafts are also common in compressional settings where a ductile unit is present at depth to fragment overburden strata (e.g. Gutscher et al., 2009). Geometrically, however, megaboudins and rafts can be similar to the submarine slide blocks referred to in this paper.

3.1 Blocks on active continental margins

Stratigraphic successions containing blocks are ubiquitous on tectonically active margins of Southern Europe and New Zealand that were uplifted during the Cenozoic. Accessible outcrop and offshore analogues include the Friuli Basin in NE Italy and Slovenia (Ogata et al., 2014), the Italian Dolomites (Brandner et al., 1991), Late Paleogene and Holocene successions in NW Italy (Migeon et al., 2011; Perroti et al., 2012), SE France (Kerckhove, 1964; Kerckhove, 1974; Campredon, 1977; Pêcher et al., 1992; Dumont et al., 2011), Sumba Island in Indonesia (Roep and Fortiun, 1996), and New Zealand (Collot and Davy, 1998; Collot et al., 2001; Lamarche et al., 2008; Goff et al., 2010) (Figs. 1, 4a and Table 1).

On the island of Crete (Eastern Mediterranean Sea), blocks occur as part of a mixed carbonate-siliciclastic succession collapsed over a tectonically active submarine slope (Fortuin, 1977; Postma et al., 1993; Ten Veen and Postma, 1999a; 1999b; Zachariasse et al., 2010; Alves and Lourenço, 2010) (Figs. 1, 3b and 4b). Blocks in SE Crete can reach ~140 m in height, and more than 100 m in length (Alves and Lourenço, 2010) (Fig. 4b).

In SE Spain, a series of transtensional basins were formed during the Late Cenozoic and filled with sediment sourced from surrounding structural highs (Haughton, 2000). This sediment was primarily redistributed by gravity flows (Kleverlaan, 1989a, 1989b; Dabrio, 1990; Haughton, 1994; Haughton 2000). As a result, schist blocks are observed in 'megabeds' of debrites around the Cautivo Fault Zone (Gordo Megabed, Tabernas Basin) and large gypsum and reefal blocks are observed at Sorbas (Martín and Braga, 1994; Fortuin and Krijgsman, 2003; Hodgson and Haughton, 2004).

3.2 Blocks on passive continental margins

Slide blocks are scarcer on passive continental margins than on active plate boundaries. Yet, some important examples are documented on passive margins around the world in association with large scale MTDs: a) offshore Norway (Haflidason et al., 2004; Bryn et al., 2005; Kvalstadt et al.,

2005), b) on the Labrador Margin (Deptuck et al., 2007), c) offshore West Iberia (Soares et al., 2014), d) on the Great Bahamas (Principaud et al., 2015), and e) in SE Brazil (Alves, 2010) (Figs. 4c, 4d and 5a).

In SE Brazil (Espírito Santo Basin), blocks occur in mixed carbonate-siliciclastic successions forming the base of the Eocene Abrolhos Formation, and within younger Late Miocene strata (Fig. 5a). Late Eocene to Holocene blocks were deposited concomitantly with the incision of submarine channel systems. Periods of tectonic inversion and salt tectonics played a significant role in slope destabilization and channel incision (Davison, 2007).

A setting comprising large volumes of blocks is that of peri-reefal areas of carbonate platforms. A recent example has been documented by Principaud et al. (2015) on the Great Bahama Bank (Fig. 1 and Table 1). Here, high-resolution multibeam bathymetry maps reveal large escarpments, 80–100 m in height, from which large carbonate MTDs with 'megablocks' were sourced during the Pliocene and Quaternary (Jo et al., 2015; Principaud et al., 2015).

3.3 Blocks associated with near-surface halokinesis

Three-dimensional seismic data are often used to assess the control of halokinetic structures on the distribution of blocks. This control is variable, depending in great part on the strength of near-seafloor strata and on the degree of deformation imposed by halokinetic structures. In the Santos Basin, SE Brazil, normal faults and folds are common within blocks, with folds typically best developed toward either the frontal or lateral margins of the clasts (Jackson, 2011) (Fig. 5b). In the Espírito Santo Basin, also in SE Brazil, deformation styles in blocks reflect distinct flow characteristics and the presence of significant seafloor topography, including other blocks (Gamboa et al., 2011). A significant observation in the Espírito Santo Basin is that the thickness of the interpreted blocks is larger on top of salt ridges, not on their flanks (Fig. 5c and 5d).

3.4 Blocky successions on the flanks of volcanic islands

In the Lesser Antilles Arc, Canary Islands and other volcanic island groups occur some of the best examples of blocks generated by flank collapse on submarine volcanoes (Mehl and Schmincke, 1999; Deplus et al., 2001; Boudon et al., 2007; Harbitz et al., 2012). On the Canary Islands, Watts and Masson (2001) and Masson et al. (2002) used sidescan sonar data to show that the north flank of Tenerife has been subjected to a minimum of four major slides during the past 1.0 Ma (Fig. 1 and Table 1). A similar setting was proposed by McGuire (2003) for the Cumbre Vieja (La Palma) and Fogo (Cape Verde) Islands.

On the flanks of the Stromboli Volcano, Casalbore et al. (2011) recognised blocks in areas associated with large-scale sector collapses capable of generating tsunami waves (Fig. 1 and Table 1). Blocks are also documented around volcanic island groups in the Indian and Pacific Oceans (Rees et al., 1993; Wolfe et al., 1994; Moore and Chadwick Jr., 1995; Labazuy, 1996; Leslie et al., 2002; Yokose and Lipman, 2004; Saint-Ange et al., 2013) (Fig. 1 and Table 1).

In Australia, the best known examples of outcropping blocks comprise Archean submarine volcanic debris, some with economic importance (Trofimovs et al., 2004). In particular, the Boorara Domain of the Kalgoorlie Terrane (Eastern Goldfields Superterrane of Western Australia) includes Archaean felsic and ultramafic breccias interpreted to reflect volcanic debris avalanche deposits, mostly dacititic in their composition, and deposited in submarine environments (Trofimovs et al., 2004) (Fig. 1 and Table 1).

3.5 Blocks on the fringes of active orogens

Back-arc basins of southern Peru, Colombia and Argentina are rich in submarine slide blocks (Fig. 1 and Table 1). In the Ayabacas region, the bulk of a mid-Cretaceous carbonate platform collapsed near the Turonian–Coniacian boundary (~90-89 Ma; Callot et al., 2008). Resulting mass-

wasting deposits, the Ayabacas Formation, include thick megabreccia deposits with heterometric clasts and blocks that are millimetric to kilometric in size. Similar cohesive slides are observed on the Sinu Accretionary Prism and the Magdalena Submarine Fan, Colombian margin, together with rubble masses up to 50 m high and runout distances between 3.6 and 11 km (Idárraga-García and Vargas, 2014).

Older slope and basin deposits in the Cow Head Group of Newfoundland contain a wide variety of carbonate 'clasts' (James, 1981) (Fig. 1 and Table 1). Among the most common, largest, and most persistent of 'clasts' are large blocks of fine-grained white limestone, middle Middle Cambrian to lower Middle Ordovician in age (Hiscott and James, 1985; Pohler and James, 1989). Paleozoic blocks are further observed in the Argentine pre-cordillera, where ~2500 m of Cambrian-Ordovician limestones (bioherms) and dolomites are observed (Fig. 1 and Table 1). Some of these bioherms are disrupted and embedded in siliciclastic units (Cañas and Carrera, 1993; Dávila and Astini, 2003; Garcia and Hérail, 2005; Callot et al., 2008).

Of economic importance are Neoproterozoic blocks and tectonic megabreccias of the Katanga Supergroup (Wendorff, 2000; Wendorff, 2011), in the interior of which Cu and Cu–Co deposits of the Central African Copperbelt are observed in association with blocks (Wendorff, 2001; 2003; 2011). Mineralised intervals inside blocks of the Katanga Supergroup are part of, or related to, banded iron formations (BIF) accumulated on a continental margin dominated by dolomites, shales and sandstones (El Desouky et al., 2009).

4. Diagnostic features of blocks at seismic scales

This section gives an account of the geological features that are typical of blocks, for the greatest part based on seismic data from SE Brazil and SE Japan (Fig. 1).

4.1 Remnant and rafted blocks generated during mass-wasting events

Remnant and rafted blocks present characteristic structural and kinematic features on 3D seismic data, and alternate in space within mass-wasting intervals. Remnant and rafted blocks generally comprise features with high reflection strength (Fig. 5c). In contrast, debrites and other mass-wasted strata are seen as low coherence strata with variable amplitude (Gamboa et al., 2011) (Figs. 5c and 5d).

Figure 5d represents a coherence slice taken 20 ms above the basal glide plane of a blocky MTD (Gamboa et al., 2011). Chaotic sections on coherence data are shown as dark, mottled patterns that record the presence of debrites. In contrast, individual blocks are clearly distinguished within these mottled areas as coherent subgeometric features with sharp edges (Fig. 5d). Remnant blocks comprise, in this same area, *in situ* elements that were not removed by erosion and mass-wasting. Remnant blocks show vertical stratigraphic continuity with underlying non-MTD strata, lacking a gliding surface (Fig. 5d).

On seismic data, the identification of remnant blocks must take into account the relationship between their edges and any underlying faults. Remnant blocks do not show basal deformation features and can be bounded by faults propagating from underlying strata (Fig. 5c). In contrast, rafted blocks are considered to have been transported downslope and commonly rest on top of the gliding surface (Fig. 5c). Some are seen 'floating' within the disaggregated chaotic matrix of the MTD, forming features associated with differential compaction above them.

4.2 Differential compaction of strata draping blocks

In SE Brazil, characteristic features of differential compaction comprise large depressions sub-parallel to the direction of transport of slide blocks, and smaller transverse depressions (Fig. 6b). Depressions in post-MTD strata can be 50-60 m deep (Alves, 2010) (Figs. 6a to 6c). Morphological data shows a scale relationship between the length and the width of such depressions, i.e. the width

of compaction-related depressions is 0.4 of their length (Figs. 6d and 6e). These scale relationships are valid in SE Brazil but might vary on continental margins depending on: a) overburden lithology and near-seafloor fluid pressure; b) block lithology and fluid content; c) degree of structural and depositional compartmentalization in blocks.

In essence, syn-depositional structures related to differential compaction include: a) local thickening of strata, particularly within chasms and regions delimited by uncompacted remnant blocks, b) small depressions generated in response to prolonged (and localised) subsidence due to compaction of failed strata (Fig. 6a). In turn, post-depositional features comprise: a) folded strata on the flanks of uncompacted remnant and rafted blocks, as opposed to a 'passive' sub-horizontal draping of debrites (Haflidason et al., 2004), b) short-wavelength folding of strata above rafted blocks in the distal part of MTDs, and c) larger-scale topographic obstacles on the palaeo-seafloor imposed by variations in relative compaction between more remobilized MTD strata and large remnant blocks (Alves, 2010). These features contrast markedly with poorly displaced headwall blocks.

4.3 Poorly displaced blocks in headwall regions

Moderately displaced blocks can be ubiquitous in headwall regions of MTDs. They form boundary scarps on the upslope margins of MTDs, or mark the most recent episodes of retrogressive failure on continental slopes (Bull et al., 2009). This work extends the concept of 'headwall scarps' to consider most of these scarps as comprising fault-bounded, and poorly displaced, blocks formed during the first stages of seafloor collapse (Area 1 in Fig. 3b). These poorly displaced blocks are a product of local failure that did not progress into a full dynamic slide. Kvalstad et al. (2005) modelled the static and dynamic conditions necessary to initiate movement in headwall blocks, concluding that unloading of the headwall is a prerequisite process. Such a phenomenon causes strain concentrations and strength loss at the basal plane, sufficient to reduce

the factor of safety (FS) below 1 and thus initiate a dynamic slide process. In turn, decreases in sensitivity, rate of softening and denudation will result in the abrupt cessation of movement if no other factors i.e., decreasing effective stress at basal glide planes and tectonic oversteepening, compensate for this softening loss (Andresen, 2001). Downslope, a contrasting geometry is observed at the lateral margins of MTDs, where blocks are ubiquitous and reflect distinct deformation styles.

4.4 Sheared blocks on lateral margins of MTDs

Lateral margins of MTDs are generated parallel to their gross flow direction, and can offer a primary kinematic constraint (Bull et al., 2009). They are chiefly associated with strike-slip movements in MTDs (Martinsen and Bakken, 1990, Martinsen, 1994), although transpressional or transtensional deformation may also occur in areas of significant seafloor roughness (Martinsen, 1994).

Alves and Cartwright (2009) showed an exception to the apparent random scattering of remnant and rafted blocks in a 1-km wide band along the lateral scarps of a MTD in SE Brazil (Fig. 8a). Here, blocks comprise more than 0.6–0.7 of the total volume of deposited strata. The authors showed the size of observed blocks to be substantially smaller towards the marginal areas of the slide due to the reduced thickness of strata remobilised in these areas when compared to proximal and central regions (Fig. 7a).

Localized dip-slip collapse of high, steep lateral scarps towards the centre of the MTD body can also occur (Varnes, 1978; Bull et al., 2009). Blocks might be present on the lateral margins of MTDs to reveal strike-slip offsets and shearing. They can also be expressed as raised, positive features due to localised or net accumulation of material in the translational or toe domains of MTDs (Trincardi and Normark, 1989). This net accumulation is chiefly recorded when displaced blocks are buttressed against slope topography, as discussed later in this paper for the SE Crete

case-study. Locally, net accumulations are also recorded on the larger ramps and fault-related topography created at the base of displaced MTDs.

4.5 Ramps and flats in basal shear surfaces

Ramps comprise segments of basal shear surfaces that cut discordantly across bedding, whereas 'flat' sections are bed-parallel segments of the basal shear surface (Lucente and Pini, 2003) (Fig. 7b). Gawthorpe and Clemmey (1985) and Trincardi and Argnani (1990) report that most ramps trend perpendicular to the main flow or movement direction, a postulate reassessed by Omosanya and Alves (2013) for salt-rich margins and by Alves et al. (2014c) for tectonically active margins.

Basal glide planes can also comprise grooves or furrows. These are long, linear or sinuous features that are 'v' shaped in cross-section (Posamentier and Kolla, 2003; Gee et al., 2005). Grooves may be continuous over many kilometres and are generally orientated or diverging downslope (Gee et al., 2005; Draganits et al., 2008). They are interpreted to result from the erosional action of coherent blocks translated downslope (Gee et al., 2005). Grooves usually follow the presence of streaks on the basal glide planes of MTDs (Bull et al., 2009), but their relevance as kinematic indicators requires a case-by-case assessment (Draganits et al., 2008).

Seafloor roughness can lead to the generation of ramps, grooves and streaks that are dissimilar in orientation to the original transport direction of MTDs. For instance, Alves et al. (2014c) showed that the direction of transport of an MTD from Nankai (SE Japan) differs 30°–45° from the strike of scarps and ramps at its base (Figs. 7b and 7c). The authors found the ramps in SE Japan to be parallel to the structural contours of thrust anticlines underneath, not to the transport direction of the interpreted MTD, a character contrasting with the geometries frequently documented in frontally emergent submarine slides (e.g. Frey-Martinez et al., 2006). Basal ramps are also associated with zones in MTDs with distinct geological properties, and show ramps and other features can be unreliable kinematic indicators. Alves et al. (2014c) postulated that the generation of basal ramps

relates to the combined effect of the erosional power of the mass-transport body and pre-existing seafloor roughness, and not solely to the transport directions of MTDs. Basal glide planes may be complex on seismic data, rather than comprising a single surface between undisturbed strata and the base of displaced blocks (Fig. 8a). This character is further discussed at the end of this paper.

An additional kinematic indicator proposed by Omosanya and Alves (2013) comprises circular and elliptical features around growing salt diapirs (Fig. 8b). These features provide evidence of local (paleo) stresses associated with compression or extension. Omosanya and Alves (2013) showed the recurrence of MTDs to vary across specific areas of elliptical 'drag zones' around growing diapirs, relating the morphology of basal shear surfaces to local strain and directions of transport during mass-wasting events (Brami et al., 2000; Lamarche et al., 2008). Sections of MTDs that were later uplifted on the flanks of growing diapirs form elongated features that are parallel to the dominant trend of basal ramps and promontories, constituting markers for seafloor strain around growing salt diapirs (Fig. 8b). Omosanya and Alves (2013) also found variations in the internal character of MTDs to occur across these same ramps and promontories, with slightly deformed, coherent, unrotated and rafted blocks alternating in space.

4.6 Internal folding, faulting and shearing in blocks

Blocks tend to be deformed by two sub-perpendicular families of vertical faults and fractures, with one family sub-parallel to the downslope gliding direction (Gamboa and Alves, 2015a). Internal shearing and folding are also pervasive in these blocks. Shear structures are observed not only at the base of the blocks but also at multiple intra-block horizontal detachment levels accompanying chasms and large faults (Fig. 9).

Chasms are formed by extensional stresses generated during minor movement of blocks (Varnes, 1978). In their work, Bull et al. (2009) suggested that proximal extensional features compare to square to rectangular blocks, or to more laterally continuous ridges separated by normal

or listric faults (e.g., Bøe et al., 2000; Frey-Martinez et al., 2006; Solheim et al., 2005). Bull et al. (2009) also postulated that blocks are typically elongate due to their association with extensional faults propagating along-strike, orthogonally to the direction of the minimum confining stress (σ_3); therefore sub-parallel to the headwall scarp (Varnes, 1978, Bøe et al., 2000, Laberg and Vorren, 2000, Frey-Martinez et al., 2006). Step-like, or 'stair-case', patterns are indicative of a retrogressive pattern of failure development (Kvalstad et al., 2005).

Large scale shearing and thrusting can occur within slide blocks, resulting in increased seal risk (Gamboa and Alves, 2015a). This risk is particularly increased when: 1) thrust faults form paths for fluid ascension, and 2) anticlines that tilt the original stratification favour upward flow along existing permeable strata (Gamboa and Alves, 2015a). These same authors found the remobilization of soft sediment along sand-rich basal intervals to favour the accumulation and injection of permeable lithologies along structural and stratigraphic discontinuities, locally enhancing the permeability of blocks. As a result, the combination of vertical and horizontal structures, alongside the original stratigraphic architecture of blocks, creates a complex deformation mesh and forms preferential fluid bypass conduits within them (Gamboa and Alves, 2015a).

5. Outcrop examples

Outcrop data from southeast Crete have shown a variety of deformation styles at the base of individual blocks (Alves and Lourenço, 2010). Deformation styles at outcrop include recumbent folding of ductile material, bed-parallel shearing, rolling of larger blocks under breccia-conglomerate carpets and moderate sliding on detachment faults. This section gives an account of their remobilisation and depositional styles based on new data from SE Crete acquired in 2011 and 2013 (Figs. 3b and 3c).

5.1 Autochthonous carbonate blocks and breccia-conglomerates denoting limited gravitational collapse

Figure 3b shows the three areas west of Ierapetra where proximal, intermediate (translational) and frontal regions of a Late Miocene blocky MTD were re-mapped. Area 1 comprises autochthonous carbonate fan cones and boulder conglomerates showing minor evidence of collapse (Fig. 3b and 10a). Here, blocks are interpreted to be authochthonous to poorly displaced. They occur mainly in proximal (upper) areas of the Miocene paleoslope (Fig. 3b).

Ravines and chasms reaching 30-m in width are observed at several locations, namely northwest and north of Anatoli (Fig. 3b). Block fragmentation occurred in the Late Miocene, with later tectonic uplift and emersion of the paleoslope contributing to the preferential erosion of fractured portions of the blocks. In Area 1, fan cones and boulder conglomerates accumulated above coarse-grained siliciclastic sediment of the Parathiri member (Fortuin, 1977, Alves and Lourenço, 2010) (Fig. 3c). In parallel, most of the Males Formation is significantly fragmented and sand blocks are observed together with carbonate megabreccias (Fig. 10b).

5.2 Disrupted deep-water (carbonate) fan cones, carbonate megabreccias, and boulder conglomerates

In Area 2, boulder conglomerates and megabreccias are unconformable above the Parathitiri Member (Figs. 3b, 3c and 10c). Blocks alternate spatially with disaggregated boulder conglomerates (Fig. 3b). These boulder conglomerates show greater disaggregation when compared to similar strata in Area 1. Structural deformation in Area 2 is, nevertheless, similar to Area 1 only with more pronounced lateral spreading of blocks (Fig. 3b).

Fan megabreccias and boulder conglomerates are visible in intermediate to distal parts of the Ierapetra paleoslope (Fig. 3b). They are chiefly composed of well-rounded, grey and black pre-

Neogene limestone clasts within calcareous silts or sands (Fortuin, 1977). Megabreccias and boulder conglomerates were deposited by debris flows sourced from proximal parts of the Ierapetra paleoslope, and from megabreccia deltas deposited in a shallow marine environment controlled by tectonic movements.

In contrast to Area 2, a large proportion of disaggregated carbonate blocks are observed on top of the Kalamavka Formation in Area 3 (Figs. 3b, 3c and 10d). Basal contacts are erosional between individual blocks and slope strata (Fig. 10e). A key characteristic of Area 3 is that strata are upturned at the front of large-scale blocks. Structural deformation is mainly concentrated at the base of rafted blocks. Blocks in Area 3 contrast with younger boulder conglomerates and fan cones by revealing a larger transport distance, and by deforming adjacent slope strata underneath and in front of them. Outcropping portions of blocks in Area 3 can also be part of large carbonate bodies buried underneath the surface, and only partly exposed.

5.3 Rotational sliding and lateral spreading of blocks and boulder conglomerates (10-100s m-scale features)

Rotational slides are chiefly observed in Area 1 at locations 2, 15, 66 and north and east of the village of Kalamavka (Figs. 3b). Rotated slabs are in the scale of tens to hundreds of metres. Beds can be subvertical at places. Evidence of rotational sliding is also observed on distal parts of carbonate fan-cone deposits (e.g., location 22, Figs. 3b and 10f). These rotational slides are local features as documented, for instance, in locations 39 and 66 (Fig. 3b).

Laterally spread blocks comprise rotational slides further separated by continuous downslope movement on a ductile substrate (e.g., Ilstad et al., 2004; Lourenço et al., 2006). On the Ierapetra paleoslope, lateral spreading contributed to the rafting of individual blocks above the Parathiri member, and within the Kalamavka Formation (Fig. 3c). The width of laterally spread blocks is

variable, reaching nearly 100 m at Agios Dimitris (location 22, Fig. 3b) but only a few tens of metres in location 32, for instance (Fig. 3b).

Lateral spreading of blocks is therefore ubiquitous on the Ierapetra paleoslope. Block disruption increased with transporting distance until the base of the paleoslope, or a bathymetric feature capable of forming a buttress, were found by the SE Crete blocks. One of such buttresses occurs in the Myrtos to Gra-Ligia corridor and led to the concentration of some of the largest blocks observed in SE Crete (Fig. 3b).

5.4 Aperture of ravines and chasms in gravitationally unstable blocks (1-10s metres)

Ravines and chasms are chiefly observed in Area 1 north of Kalogeri and Kalamavka, and in Area 3 where they are widened by preferential weathering and erosion along split blocks (Figs. 3b and 11g). The scale of such features varies from <1 m to 30-40 m in width. The aperture of ravines and chasms was most likely initiated in a submarine environment i.e., during the Tortonian-earliest Pliocene. Further subaerial erosion and slope instability led to continuous fragmentation of blocks, and emphasised the presence of chasms (Fig. 10g).

Ravines and chasms reflect a later stage of slope instability, likely associated with slow block movement and internal fracturing. Some chasms are, at present, wider than originally due to subaerial erosion of blocks exposed during the Quaternary.

5.5 Rockfalls (1-10s m) of fractured blocks

Rockfalls from fractured blocks are chiefly modern events but are believed to have also occurred during the collapse of the Ierapetra palaeoslopes. Fallen rocks are observed together with fragmented blocks in Areas 2 and 3 (Fig. 3b). They reach 20 m in length, being in average less than 10 m in diameter. However, fallen blocks embedded in the Kalamavka, Makrilia and Ammoudhares

Formations, and toppled adjacently to larger Miocene blocks, are interpreted as relating to the fragmentation of larger blocks.

5.6 Sliding and rolling of blocks (10s metres) over a ductile basal layer

Blocks reflecting large-distance transport are scattered throughout the southern parts of Areas 2 and 3 (Fig. 3b). They consist of 10-60 m long blocks showing basal deformation structures (Fig. 10h). In these areas, the collapse of blocks occurred mainly over the Parathiri Member and Kalamavka Formation (Fig. 3c). The scale of blocks in Areas 2 and 3 varies from 10 to 100 m, with individual blocks >100 m in length being visible at specific locations (locations 38 and 39, Fig. 3b). This style of failure is diagnostic of submarine slope environments and is better observed: a) within strata of the Kalamavka Formation, and b) close to the contact between the Makrilia and Ammoudhares Formations (Fig. 3c).

Often embedded within a debris-flow matrix at the base of the Prina Group, rolled subcircular blocks appear scattered within the Males, Kalamavka and Makrilia Formations (Figs. 3b and 3c). They comprise polymictic breccia-conglomerates and siliciclastic (sandy to conglomeratic) blocks in the Males Formation. Rolled blocks reach tens of metres in diameter, but are normally measured in decimetres or metres.

6. Soft-sediment kinematic indicators

In SE Crete, blocks present kinematic indicators that are of interest in understanding the physics and directions of past mass movements. Most of the kinematic structures observed in outcropping blocks reflect transport styles such as: a) gliding; b) block drag and skipping; c) toppling; d) free fall; and e) translation over high-density megabreccia flows. They are associated with earthquake activity, sediment liquefaction and block sinking into background slope strata. Other structures

represent post-depositional tectonic deformation and block remobilisation on a tectonically oversteepened slope, as pointed out by Fortuin (1977), Fortuin and Peters (1984) and Postma et al. (1994).

Of particular importance to this work are kinematic indicators with curved shape or offset geometries that indicate the sense of shear directly from their observation in the field. These kinematic markers occur below displaced blocks and reflect ductile conditions within water-filled sediment, as recognised (but not fully explained) in Mills (1983). Soft-sediment kinematic indicators in SE Crete are described in detail in the following sub-sections.

6.1 Slide foliation

Foliation is defined as the planar arrangement of structural or textural features in any rock type, and results from compression or shearing in distinct directions. Foliation generates planes of anisotropy in ductile strata (Platt and Vissers, 1980; Dell'Angelo and Tullis, 1988). As a result, foliation and cleavage further increase the ductility of sheared material in specific orientations so that brittle fractures or shear bands are able to develop (Platt and Vissers, 1980).

Underneath the larger blocks in SE Crete are observed coarse foliation and laminae in shaley and silty horizons (Figs. 11a and 11b). These low-temperature, low-pressure structures are primarily formed in a ductile substrate under the weight of moving blocks. They are often accompanied by soft-sediment shear structures that can be used as reliable kinematic indicators (Fig. 11a). Clays and silts show some degree of compositional banding, mostly primary banding emphasising the presence of strata disrupted under the weight of downslope moving blocks (Figs. 11a and 11b).

6.2 Pull-apart structures, dilational jogs and associated tear faults

Pull-apart structures are associated with geometric and possibly mechanical irregularities in faults crossing glide planes (Aydin and Nur, 1982). During the blocks' motion, releasing or restraining bends of faults resulted in the creation of dilational jogs and horses at variable scales. The most reliable kinematic indicators in SE Crete are small rotational faults and pinch-and-swell geometries observed in cemented pull-apart structures formed under the weight of moving blocks (Fig. 11c). In Figure 11c are shown examples of pull-apart structures under a displaced block revealing a transporting direction to the East. These structures generally accompany the foliation of clayey and silty sediments. Their generation was followed by the formation of calcite veins, a character suggesting the presence of carbonate-rich fluids below the displaced blocks. These fluids were likely overpressured within the deformed interval that forms the basal glide plane.

A distinct type of pull-apart structures are dilational jogs, which are frequently observed in thin-bedded strata,. At Agios Dimitrios (location 22), they are accompanied by tear fractures and Riedel shears, 80-100 cm long, that follow the transport direction of a block quarried above the glide plane (Fig. 11d). Individual beds were pulled apart and fractured in a direction similar to the transporting direction of the block, as estimated by foliation and fold geometries (Fig. 11d and 12b). The resulting dilational jogs are interpreted as a response to the weight and dragging of blocks on the top of laminated fine-grained strata. Such a process occurred in a brittle regime that is likely to be associated with the terminal stages of block movement.

6.3 Intrafolial folds

Folding is related with the buckling of anisotropic strata in a specific direction (Cobbold et al., 1971). In Ierapetra, folds are common in specific intervals below individual blocks, occurring either as recumbent folds, asymmetric folds, quarter folds or accompanying sediment liquefaction and deformation in specific intervals underneath the blocks (Fig. 11e). Often, folds are visible in the first couple of metres below collapsed blocks, and are intercalated with more chaotic strata

comprising sandy and silty material injected during the basal deformation event (Fig. 11e). Fold axial planes tend to be parallel to the transporting direction in recumbent folds, but are apparently random when associated with specific sandy-silty horizons denoting liquefaction. This character grants them as unreliable kinematic indicators, unless they are complemented with secondary indicators such as dilational jogs, fractures and pull-apart geometries. Asymmetric and quarter folds are commonly found in intervals with recumbent folds (Fig. 11e).

6.4 Tiling structures, stretched clasts, imbricated strata and bookshelf sliding

Rotational faulting (bookshelf sliding) in beds, tiling structures and imbricated strata indicate bed-parallel extension or compression during block movement and slope collapse. Bookshelf sliding reflects fault rotation by external shear as defined in Mandl (2000). Imbricated clasts, stretched clasts and tiling structures indicate rotation and local shear (Fig. 11f). Tiling structures and boudins are mostly strained and rotated in the direction of transport of the blocks.

Structural measurements of tiling and imbricated structures indicate a SSE to SE transport direction at Kalamavka and Agios Dimitrios, in Area 2 (Fig. 3b). These directions are consistent for individual blocks, but vary when analysing different blocks along the Mirtos-Ierapetra zone (Area 3), where they denote a N-S direction of collapse (Fig. 3b). Rotational faulting of beds and imbrication of strata parallel to bedding are also observed in stratified successions below collapsed blocks.

6.5 Thrusting and foliation in frontally confined MTDs of SE Crete and Almeria (Spain)

In the region extending from Mirtos to Gra-Ligia, large blocks pushed, upturned and folded the Kalamavka, Makrilia and Ammoudhares Formations (Figs. 3c and 12a). The series of thrusts and large-scale recumbent folds observed in this area denote a predominant north- to south-direction of

compression that is associated with the gravitational collapse of the Ierapetra palaeoslope along a region 5-km long by <1 km wide (Fig. 3b). Folding is particularly observed at location 43, where large recumbent folds, approximately 15 m high and with a >50 m crest, deform slope strata in the Kalamavka and Makrilia Formations (Fig. 12b). Folding of strata belonging to the top of the Makrilia Formation, with the Ammoudhares Formation resting on top of the beds as a south-facing monocline, indicates that part of the frontal thrusting is late Tortonian-early Messinian in age.

In Miocene strata from the Tabernas Basin, SE Spain, MTDs are seen to ramp-up pre-existing topography in a style similar to frontally-confined slides in Frey-Martinez et al. (2006) (Fig. 12c). Frontal thrusting is here a reliable kinematic indicator, but only if the ramp is perpendicular to the transport direction of the MTD. Once again, local structures denoting shearing and pull-apart are observed at the extensional part of the MTD are more reliable kinematic indicators, as they respond to the evacuation of displaced material, rather than to the geometry of the ramp below (e.g. Alves et al., 2014c) (Fig. 12d).

7. Discussion

Numerical models of block formation and movement provided for the Norwegian margin by Bryn et al. (2005) and Kvalstadt et al. (2005) consider three main factors controlling the geometry of submarine slide blocks: slide mechanism, excess pore pressure and strain softening. Pressure build-up at the base of large scale blocks is another important control on their movement (Fig. 13). Triggers inducing this pressure build-up include: a) earthquake induced shear strain generating excess pore pressure; b) melting of gas hydrates releasing methane gas and water, c) shear strain induced contraction with pore pressure generation and softening during the slide process causing progressive failure and retrogressive sliding, and d) rapid deposition (Kvalstadt et al., 2005). Any of these triggers, or any combination of the four, can induce block collapse and movement in a style

resembling retrogressive failure over quick-clays (Fig. 13). In the following sections are discussed key aspects of blocks on multiple geological settings.

7.1 Pre-conditioning factors for the generation of submarine slide blocks

One key observation from this work is the marked similarity between blocky successions in SE Spain and SE Crete in terms of their tectono-sedimentary evolutions. This similarity is revealed by their common basin fill, with blocks and collapsed slope strata alternating with turbidite intervals (Fortuin, 1977; Postma et al., 1993; Postma and Drinia, 2003; Dabrio, 1990; Haughton, 1994; 2000) (Fig. 13). In addition, the predominance of faulting, laminations and imbrication at different scales of observation, metre- to millimetre-scale, suggests the stratified successions in the field analogues to be part of a sheared interval i.e., not representing true bedding. Most of the varve-like successions observed below slide blocks are, therefore, centimetre to millimetre-scale sheared strata, rotated and foliated to form alternate sets of silt and shales, all part of a complex glide plane. Examples are shown in Figs. 11a and 11b, where foliated strata is truncated and eroded by mobile intervals that were displaced and deformed below moving blocks. This structure occurs ubiquitously below displaced blocks in SE Crete.

A similar stratigraphic record to SE Crete and Spain was observed in Peru by Callot et al. (2008), and explained as deriving from instability phenomena taking place in two-layer environments made of different materials. Thus, siliciclastic sediments in Peru, SE Spain and SE Crete were deformed in plastic and plastic-viscous rheological states, whereas the absence of similar features in blocks suggests they were deforming elastically, because the material behaved brittle. Such an observation corroborates data from outcropping slope deposits around the world, over which: i) siliciclastic materials were in a plastic-viscous state during the gravitational collapse of blocks, ii) blocks were kept relatively undeformed, even when transported long distances, and iii)

the presence of clay in the matrix of blocks is recorded at outcrop, and contributed to maintain their internal cohesion when transported downslope.

The bi-modal lithological distribution documented in Crete and Spain is considered in this work to be a primary pre-conditioning factor for the generation of blocks. Blocks are only kept intact, regardless of their lithology, when they maintain their internal cohesion in a ductile, soft glide plane. Kvalstad et al. (2005) recognised in Norway that a two-layered structure is associated with the build-up of pore pressure near the seafloor, thus predisposing slope strata to fail. If near-seafloor lithology is more homogeneous, submarine slides will be devoid of blocks, more recurrent, and alternating with turbidite successions such as those of SE Japan and SE Spain (Kleverlaan, 1987; Dabrio, 1990; Haughton, 1994; 2000; Strasser et al., 2011; Alves et al., 2014c).

A secondary pre-conditioning factor is the presence of sandy material at the base of large blocks (Alves and Lourenço, 2010). The seismic shaking of loose granular sediments beneath the blocks can cause sands in these units to densify. With no time for water to dissipate, pore water pressures in excess of the hydrostatic are generated, leading to a reduction in the effective stresses (e.g., Allen, 1982; Owen, 1987; Nichols, 1995; Powrie, 2002). These conditions are sufficient to initiate block movement, eventually leading to liquefaction of underlying sands if seismic shaking intensifies (Lourenço et al., 2006). An immediate consequence of such a process would be the sliding, sinking and partial burial of blocks in sandier slope strata, as observed at Ierapetra.

A third likely trigger of blocks in SE Crete and SE Spain includes the accretion of carbonate material on the palaeoslope as a result of its continuous (tectonic) steepening with time. In this case, failure would start when the downward component of the weight of the blocks exceeds the resistive vertical component (Fig. 13). Retrogressive failure leading to large run-out distances was sufficient a process to push large slide masses over ramps and steps formed in the slip surface, increasing the kinetic energy of blocks and their resulting fragmentation (Kvalstad et al., 2005; Micallef et al., 2007) (Fig. 13).

7.2 Structural and geotechnical parameters controlling block displacement

Basal slip planes of subaerial slides occur at scales below 1.0 m, and usually comprise weak strata with particular geotechnical properties, such as plastic shales, undercompacted layers (lithological bands), and permeable layers subjected to fluid flow. Also important are weakness planes in rocky formations e.g., lithogenetic fissures, fractures due to unloading of a rock massif and tectonic faults (Shibakova et al., 1977; Nemec, 1990; Gamboa and Alves, 2015a). Glide planes of onshore slides are known to form in essentially brittle regimes of deformation (Alves and Lourenço, 2010). They respond to topographic features, either through damming of material in areas of topographic constriction, or can accelerate and liquefy basal glide plane strata if slopes are broad and become steeper with block's transporting distance (Lucente and Pini, 2003; Hodgson and Houghton, 2004).

An important observation in SE Crete is that outcropping blocks were translated above polymictic breccias, and other deformed strata, i.e. within an interval that includes remobilised clasts sourced from basal strata in the blocks (Figs. 10d and 15a). Rolled and translated limestone clasts occur within these polymictic breccias, which are often embedded in the interior of a clayey matrix (Fig. 10d). This complex structure puts in question the morphology of basal glide planes as interpreted on seismic data (Figs. 8a and 9). Blocks, polymictic breccias and (paleo) seafloor strata are, at outcrop, deformed together (Fig. 14). In addition, areas with deformed basal strata abruptly change into an undeformed stratified succession a few meters below the base of the collapsed blocks (Fig. 14). Such a boundary can be mapped as the base of MTDs on seismic data, but *de facto* materialises the contact between deformed and intact slope strata below failed slope deposits (Figs. 8a and 9).

The ratio between the thickness of failed deposits and the corresponding thickness of deformed strata at the base of the blocks (R) was found to be in the order of $5 < R < 10$ (Alves and Lourenço, 2010). A linear regression shows that T_{BSZ} (thickness of the basal shear) is approximately 0.15 of

the height of slide blocks (H), and indicates that interpreted basal surface is rather a *basal shear zone* than a simple surface, or gliding plane (Fig. 15). This latter characteristic contrasts with subaerial slides, which take place in strata that are in comparison stiffer and show relatively high degrees of compaction, exhibiting a brittle behaviour during shear (Varnes, 1978; Gerb and Weisenfluh, 1996). The distinct behaviour of subaerial slides results in well-defined shear zones, with the thickness not exceeding scales of a few centimetres in clays (e.g., Anson and Hawkins, 1999) and involving a deformation zone not exceeding 1.5 m (Shuzui, 2001).

7.3 Key structural markers of block movement

Despite observed differences in the relative abundance of blocks in SE Crete and Spain, there are primary characteristics that are common to the two regions. The main large-scale structural marker observed in both regions is the buttressing of folded and upturned strata against older units deposited well below the (water) depth in which blocks were firstly fragmented (Fig. 16). This buttressing (and folding) is a diagnostic feature of block transport on continental slopes, along with ramping and imbrication of blocks, as shown in SE Brazil by Gamboa et al. (2011).

In the case of SE Crete, strata in the Kalamavka Formation is folded, but the Makrilia and Ammoudhares units are only slightly tilted, indicating a late Tortonian movement for most of the blocks in SE Crete (Fig. 12a). The second large-scale marker of block collapse is the angular contact formed below displaced blocks and separating these from background slope strata – recorded by the regional unconformity between slope strata of the Kalamavka/Makrilia Formations and conglomerates and megabreccias at the base of blocks in SE Crete (Fig. 10c). Such a characteristic demonstrates the presence of a tectonically active setting, with blocks and associated MTDs draping a fault-bounded, deforming slope (Figs. 3b and 10c). Slope collapse continued after this initial erosional event in multiple phases of block collapse and megabreccia transport onto the toe of the Ierapetra paleoslope (Alves and Lourenço, 2010).

Multiple phases of slope collapse can therefore be interpreted at Ierapetra, and other paleoslopes containing submarine slide blocks (e.g. Dumont et al., 2011; Wendorff, 2011). A first phase of slope instability occurred in the early Tortonian in SE Crete during the deposition of the Prina series (Fortuin, 1977; Postma et al., 1993). Relief steepening at the end of the Tortonian led to a second phase of block collapse, marked by the inclusion of blocks within the upper part of the Kalamavka Formation and by the apparent buttressing of blocks against major faults. This event contributed to the thrusting, recumbent folding, and bed upturning observed in the Mirtos-Gra Ligia corridor (Figs. 3b, 12a and 12b). Proximal blocks were kept relatively intact and do not appear to have travelled more than a few tens of metres downslope (Fig. 10a). In contrast, blocks embedded in the Kalamavka Formation were responsible for base-of-slope thrusting and were likely originated in large-scale instability events (Figs. 12a, 12b and 16).

7.4 Fluid flow through displaced and remnant blocks

On the Miocene paleoslopes of SE Crete, block distribution hints at their quick collapse and fragmentation. Multiple structures are observed at outcrop, with intra-raft shearing and important dilational faults caused by buckling of strata over paleoseafloor topography comprising the most obvious features in mapped blocks. Similar faults to Crete's are observed within large blocks of SE Brazil, many of which propagate from basal fault families that cross the entire pre-block succession (Figs. 17a and 17b). Using the height of the blocks as a proxy for the position of the paleoseafloor, this work estimates that ~400 metres of near-seafloor sediment were transported downslope in the SE Brazil seismic case-study. This event reflects a relatively quick slide event, as the blocks are passively draped by hemipelagites (Figs. 17a and 17b).

Leakage tendency was modelled across the largest of the interpreted blocks for average pore pressures of <10 MPa, i.e. for a pore pressure approaching that of a relatively shallow reservoir such as the Golfinho Field, located just below the study area of SE Brazil. Model results also

provided estimates of: a) thresholds of near-seafloor erosion beyond which a significant leakage is estimated for specific slide events; b) the main fluid paths in which fluid flow occurs prior and after slope failure. As shown in Fig. 17, this sudden erosional event compromises seal competence in the region considered in the model. The model results show that flanking scarps, faults and chasms remain as the features with the largest leakage potential in the blocks, even when buried at depths below 4000 metres (Fig. 17). Thus, faults offsetting individual blocks, and their flanking scarps, are structures that impose significant vertical anisotropy in slope strata, with the bulk of fluid flow being focused by vertical and horizontal shear intervals in the interior, flanks and base of blocks (Fig. 17).

A final result of the modelling is that the erosion of ~400 m of near-seafloor sediment, itself reflecting the complete loss of the equivalent of 5 Myr of sediment based on the positions of key unconformities on seismic data (Alves, 2012), has a significant effect on underlying petroleum systems by triggering the sudden release of vertical confining pressure above existing structural traps. Therefore, slide blocks are presented in this paper as important geological features on continental margins, because (1) they mark sudden events of slope instability on continental margins; (2) they result in the sudden loss of vertical confining pressure in underlying reservoirs; and (3) they can be related to important hiatuses and unconformities on continental margins, which are difficult to correlate across a continental slope due to the irregular character of basal shear zones and of the strata they cross.

8. Conclusions

Submarine slide blocks are important features on continental margins as they mark sudden events of slope instability, and result in the sudden loss of vertical confining pressures in underlying reservoirs. The results in this work can be summarised as follows:

a) Blocks are common in tectonically active settings, often comprising carbonates, cemented siliciclastics and other hardened lithologies in finer-grained slope successions. They are particular common adjacently to large-scale tectonic structures and flanking active volcanoes, or are associated with fluid-related slope instability. Peri-reefal and volcanic slopes are also prone in blocks with distinct lithologies.

b) Blocks and tectonic megabreccias can contain important mineralisation, such as in the Co-Cu rich Fungurume Group of Congo and Zaire.

c) Common characteristics in submarine slide blocks include the presence of key structural features at seismic scales, chasms, faults and horizontal shear planes. These form the main features controlling fluid flow in between, hard cohesive (or cemented) strata in blocks.

d) Specific remobilisation styles are observed at outcrop, such as the alternation in space of autochthonous blocks, *in situ* breccia-conglomerates with disrupted deep-water fan cones, and laterally spread blocks. These structures can form important compaction-related structural traps in overlying strata if buried at significant depths.

e) Soft-sediment kinematic indicators are varied at outcrop, with pinch-and-swell structures, dilational jogs, stretched clasts and imbricated clasts comprising the most reliable.

As a corollary of this work, it is recognised that soft-sediment kinematic indicators are important to assess the degree of internal deformation in blocks, and the style(s) of deformation of the intervals in which they occur. In addition, they can be reliable diagnostic features to understand the direction(s) of displacement of blocks. Future work should focus on the analysis of blocky MTDs as successions of enhanced permeability and porosity using indirect geophysical methods, as

they can comprise the preferential *loci* for hydrocarbon and mineral accumulations of economic importance.

Acknowledgements

The author acknowledges the permission conceded by CGG for the publication of this research paper and the personal invitations of T. Horscroft and O. Catuneanu to produce this work. The paper used SWRI 3D Stress® to model leakage factor across rafted blocks. A special acknowledgement goes to Tore Kvalstad for providing Figure 13. V. Lykousis (HCMR), I. Zananiri, N. Carras and K. Perissoratis (IGME–Athens) are acknowledged for permits to the field campaigns in Crete through 2008, 2009 and 2013. G. Postma, G. Waldron, A. Fortuin and JMPG associate editor Willem Langenberg are acknowledged for their constructive comments. This work was partly sponsored by Royal Society grant RSSV 2008/R3 and TEPA's (Total-Angola) RAFTS consortium.

References

Allen, J.R.L., 1982. Sedimentary Structures: Their Character and Physical Basis, Vol. II, Elsevier, Amsterdam, 663 pp.

Alfaro, E., Holz, M., 2014. Seismic Geomorphological Analysis of Deepwater Gravity-driven Deposits on a Slope System of the southern Colombian Caribbean Margin. Marine and Petroleum Geology, 57, 294–311.

Alves, T.M., 2010. 3D Seismic examples of differential compaction in mass-transport deposits and their effect on post-failure strata. Marine Geology, 271, 212-224.

Alves, T. M., 2012. Scale-relationships and geometry of normal faults reactivated during gravitational gliding of Albian rafts (Espírito Santo Basin, SE Brazil). Earth and Planetary Science Letters, 331-2, 80-96. (10.1016/j.epsl.2012.03.014)

Alves, T. M., Cartwright, J. A., 2009. Volume balance of a submarine slide in the Espírito Santo Basin, offshore Brazil: quantifying seafloor erosion, sediment accumulation and depletion. Earth and Planetary Science Letters 288(3-4), 572-580.

Alves, T.M., Elliott, C., 2014a. Fluid flow during early compartmentalisation of rafts: A North Sea analogue for divergent continental margins. Tectonophysics, 634, 91-96.

Alves, T.M., Kurtev, K., Moore, G.F., Strasser, M., 2014b. Assessing the internal character, reservoir potential and seal competence of mass-transport deposits using seismic texture: a geophysical and petrophysical approach. American Association of Petroleum Geologists Bulletin, 98, 793-824.

Alves, T.M., Lourenço, S.D.N., 2010. Geomorphologic features related to gravitational collapse: Submarine landsliding to lateral spreading on a Late Miocene–Quaternary slope (SE Crete, eastern Mediterranean). Geomorphology, 123, 13-33.

Alves, T.M., Strasser, M., Moore, G., 2014c. Erosional features as indicators of thrust fault activity (Nankai Trough, Japan). Marine Geology, 356, 5–18.

Andresen, L., 2001. Effect of strain softening on stability analyses. Analysis of retrogressive sliding due to strain softening - Ormen Lange case study. NGI report No. 521001-10, 29.03.2001.

Anson, R., Hawkins, A. 1999, Analysis of a sample containing a shear surface from a recent landslip, south Cotswolds, UK. Géotechnique, 49, 33-41.

Apotria, T., Lindholm, R., Metner, W., Eze, M., Gunn, D., Geslin, J., Rumelhart, P., Goulding, F., Mitchell, S., 2004. Volume interpretation of shelf collapse processes and Biafra 'disturbed' reservoirs, Eastern Niger Delta Joint Venture. AAPG International Conference, Cancun, Mexico.

Aydin, A., Nur, A., 1982. Evolution of pull-apart basins and their scale independence. Tectonics, 1, 91-105.

Barker, P.F., 1983. Tectonic evolution and subsidence history of the Rio Grande Rise. In: Barker, P.F., Carlson, R.L., Hohnson, D.A. (eds). Initial Reports of the Deep Sea Drilling Program, 72, U.S. Government Printing Office, Washington, pp. 953–976.

Barker, P.F., R.T. Buffler and L.A. Gambôa, 1983. A seismic reflection study of the Rio Grande Rise, in P.F. Barker, R.L. Carlson and D.A. Hohnson, eds, Initial Reports of the Deep Sea Drilling Program, 72: Washington, U.S. Government Printing Office, 499-517.

Berthé, D., Choukroune, P., Jezougo, P., 1979. Orthogneiss, mylonite and non-coaxial deformation of granites: The example of South Armorican Shear Zone. Journal of Structural Geology, 1, 31-42.

Blair, T.C., McPherson, J.G., 1999. Grain-Size and Textural Classification of Coarse Sedimentary Particles. Journal of Sedimentary Research, 69, 6-19.

Blenkinsop, T.G., Treloar, P.J., 1995. Geometry, classification and kinematics of S-C fabrics. Journal of Structural Geology, 17, 397-408.

Bøe, R., Hovland, M., Instanes, A., Rise, L., Vasshus, S., 2000. Submarine slide scars and mass movements in Karmsundet and Skudenesfjorsden, southwest Norway: morphology and evolution. Marine Geology, 167, 147-165.

Bøe, R., Bellec, V.K., Rise, L., Buhl-Mortensen, L., Chand, S., Thorsnes, T., 2012. Catastrophic fluid escape venting-tunnels and related features associated with large submarine slides on the continental rise off Vesterålen–Troms, North Norway. Marine and Petroleum Geology, 38, 95-103.

Borgomano, J.R.F., 2000. The Upper Cretaceous carbonates of the Gargano-Murge region, southern Italy: A model of platform-to-basin transition. American Association of Petroleum Geologists Bulletin, 84, 1561-1588.

Bosellini, A., Neri, C., Luciani, V., 1993. Platform margin collapses and sequence stratigraphic organization of carbonate slopes: Cretaceous–Eocene, Gargano Promontory, southern Italy. Terra Nova, 5, 282-297.

Boudon, G., Le Friant, A., Komorowski, J.-C., Deplus, Ch., Semet, M.P., 2007. Volcano flank instability in the Lesser Antilles Arc: Diversity of scale, processes, and temporal recurrence. Journal of Geophysical Research: Solid Earth, 112, B8, doi: 10.1029/2006JB004674.

Brami, T.R., Tenney, C.M., Pirmez, C., Holman, K.L., Archie, C., Heeralal, S., Hannah, R., 2000. Late Pleistocene deepwater stratigraphy and depositional processes offshore Trinidade & Tobago using 3D seismic data. In: Weimer, P., Slatt, R.M., Coleman, J.L., Rosen, N., Nelson, C.H., Bouma, A.H., Styzen, M., Lawrence, D.T. (eds.), Global deep-water reservoirs: Gulf Coast Section - SEPM Foundation Bon F. Perkins 20th Annual Research Conference, p. 402-421.

Briner, J.P., Miller, G.H., Davis, P.T., Bierman, P.R., Caffee, M., 2003. Last Glacial Maximum ice sheet dynamics in Arctic Canada inferred from young erratics perched on ancient tors. Quaternary Science Reviews, 22, 437-444.

Brown, A.R., 2004. Interpretation of three-dimensional seismic data, 6th ed. American Association of Petroleum Geologists, Memoirs, 42.

Bruhn, C.H., Waler, R.G., 1997. Internal architecture and sedimentary evolution of coarse-grained, turbidite channel-levee complexes, Early Eocene Regência Canyon, Espírito Santo Basin, Brazil. Sedimentology, 44, 17-46.

Bruso, J.M.. Jr., Getz, S.I., Wallace, R.L., 2004. Geology will support further discoveries in the Gulf of Guinea's Golden Rectangle. Oil and Gas Journal, 30-38.

Bryn, P., Berg, K., Forsberg, C.F., Solheim, A., Kvalstad, T.J., 2005. Explaining the Storegga Slide. Marine and Petroleum Geology, 22, 11-19.

Bull, S., Cartwright, J., Huuse, M., 2009. A review of kinematic indicators from mass-transport complexes using 3D seismic data. Marine and Petroleum Geology, 26, 1132-1151.

Callot, P., Sempere, T., Odonné, F., Robert, E., 2008. Giant submarine collapse of a carbonate platform at the Turonian–Coniacian transition: The Ayabacas Formation, southern Peru. Basin Research, 20, 333-357.

Cañas, F., Carrera, M., 1993. Early Ordovician microbial-sponge-receptaculitid bioherms of the Precordillera, western Argentina. Facies, 29, 169-178.

Campredon, R., 1977. Les formations paléogènes des Alpes maritimes francoitaliennes. Memoire H. S. Soc. Geol., France, 199 pp.

Chang, H.K., Kowsmann, R.O., Figueiredo, A.M.F., Bender, A.A., 1992. Tectonics and stratigraphy of the East Brazil Rift System: an overview. Tectonophysics, 213, 97-138.

Clayton, C.A., Cohen, M.F., Anis, M., Cooley, T.W., Honarpour, M.M., Wallace, J.P., Chambers, M.R., 1998. Ubit field rejuvenation: A case history of reservoir management of a giant oil field, offshore Nigeria. Society of Petroleum Engineers Annual Technical Conference and Exhibition, SPE Paper 49165, 16 p.

Cloos, M., Shreve, R.L., 1988a. Subduction-channel model of prism accretion, melange formation, sediment subduction, and subduction erosion at convergent plate margins: 1. Background and description. Pure and Applied Geophysics, 128, 455-500.

Cloos, M., Shreve, R.L., 1988b. Subduction-channel model of prism accretion, melange formation, sediment subduction, and subduction erosion at convergent plate margins: 2. Implications and discussion. Pure and Applied Geophysics, 128, 501-545.

Cobbold, P.R., Cosgrove J.W., Summers J. M., 1971. The development of internal structures in deformed anisotropic rocks. Tectonophysics 12:23–53.

Collot, J.-Y., Davy, B., 1998. Forearc structures and the tectonic regimes at the oblique subduction zone between the Hikurangi Plateau and the southern Kermadec margin, Journal of Geophysical Research, 103, 623–650

Collot, J.-Y., Lewis, K., Lamarche, G., Lallemand, S., 2001. The giant Ruatoria debris avalanche on the northern Hikurangu margin, New Zealand: Result of oblique seamount subduction. Journal of Geophysical Research, 106, B9, 19271-19297.

Cowan, D.S., 1985. Structural styles in Mesozoic and Cenozoic mélanges in the western Cordillera of North America. Geological Society of America Bulletin, 96, 451-462.

Dabrio, C.J., 1990. Fan-delta facies associations in the late Neogene and Quaternary basins of southeastern Spain. Special Publications of the International Association of Sedimentologists, 10, 91-111.

Dávila, F.M., Astini, R.A., 2003. Early Middle Miocene broken foreland development in the southern Central Andes: evidence for extension prior to regional shortening. Basin Research, 15, 379-396.

Davison, I., 2007. Geology and tectonics of the South Atlantic Brazilaian salt basins. Geological Society, London, Special Publications, 272, p. 345-359.

De Blasio, F.V., Engvik, L.E., Everhøi, A., 2006. Sliding of outrunner blocks from submarine landslides. Geophysical Research Letters, 33, doi: 10.1029/2005GL025165.

Demercian, S., Szatmari, P., Cobbold, P.R., 1993. Style and pattern of salt diapirs due to thin-skinned gravitational gliding, Campos and Santos basins, offshore Brazil. Tectonophysics, 228, 393-433.

Deptuck, M.E., Mosher, D.C., Campbell, D.C., Hughes-Clarke, J.E., Noseworthy, D., 2007. Along slope variations in mass failures and relationships to major Plio-Pleistocene morphological elements, SW Labrador Sea. In: Lykousis, V., Sakellariou, D., Locat, J. (eds). Submarine Mass Movements and Their Consequences, Springer, p. 37-45.

Deplus C., Le Friant A., Boudon G., Komorowski J-C., Villemant B., Harford C., Ségoufin J, Cheminée J-L., 2001. Submarine evidence for large-scale debris avalanches in the Lesser Antilles Arc. Earth and Planetary Science Letters, 192, 145-157.

Dell'Angelo, L.N., Tullis, J., 1988. Experimental deformation of partially melted granitic aggregates. Journal of Metamorphic Geology, 6, 495-515.

Diaz-del-Rio, V., Somoza, L., Martinez-Frias, J., Mata, M.P., Delgado, A., Hernandez-Molina, F.J., Lunar, R., Martin-Rubi, J.A., Maestro, A., Fernandez-Puga, M.C, Leon, R., Llave, E., Medialdea, T., Vazquez, J.T., 2003. Vast fields of hydrocarbon-derived carbonate chimneys related to the accretionary wedge/olistostrome of the Gulf of Cadiz. Marine Geology, 195, 177-200.

Di Francesco, L., Fabbi, S., Santantonio, M., Bigi. S., Poblet, J., 2010. Contribution of different kinematic models and a complex Jurassic stratigraphy in the construction of a forward model for

the Montagna dei Fiori fault-related fold (Central Apennines, Italy). Geological Journal, 45, 489-505.

Draganits, E., Schlaf, J., Grasemann, B., T. Argles, 2008. Giant submarine slide grooves in the Neoproterozoic/Lower Cambrian Phe Formation, northwest Himalaya: Mechanisms of formation and palaeogeographic implications. Sedimentary Geology, 205, 126-141.

Drzewiecki, P.A., Simó, J.A., 2002. Depositional processes, triggering mechanisms and sediment composition of carbonate gravity flow deposits: examples from the Late Cretaceous of the south-central Pyrenees, Spain. Sedimentary Geology, 146, 155-189.

Duffield, W., Stieltjes, L., Varet, J., 1982. Huge slide blocks in the growth of Piton de la Fournaise, La Reunion and Kilauea Volcano, Hawaii. Journal of Volcanology and Geothermal Research, 12, 147–160.

Dumont, T., Schwartz, S., Guillot, S., Simon-Labric, T., Tricart, P., Jourdan, S., 2012. Structural and sedimentary records of the Oligocene revolution in the Western Alpine arc. Journal of Geodynamics, 56-57, 18-38.

Dunlap, D.B., Wood, L.J., Moscardelli, L.G., 2013. Seismic geomorphology of early North Atlantic sediment waves, offshore northwest Africa. Interpretation, 1, SA75-SA91. doi: 10.1190/INT-2013-0040.1.

Dunlap, D.B., Wood, L.J., Weisenberger, C., Jabour, H., 2010. Seismic geomorphology of offshore Morocco's east margin, Safi Haute Mer area. American Association of Petroleum Geologists Bulletin, 94, 615-642.

Edwards, M.B., 2000. Origin and Significance of Retrograde Failed Shelf Margins; Tertiary Northern Gulf Coast Basin. Gulf Coast Association of Geological Societies Transactions, 50, 81-93.

El Desouky, H.A., Muchez, P., Cailteux, J., 2009. Two Cu–Co sulfide phases and contrasting fluid systems in the Katanga Copperbelt, Democratic Republic of Congo. Ore Geology Reviews, 36, 315-332.

Embley, R.W., 1980. The role of mass transport in the distribution and character of deep ocean sediments with special reference to the North Atlantic: Marine Geology, 38, p. 23-50.

Emmerich, A., Zamparellu, Bechstädt, T., Zühlke, R., 2005. The reefal margin and slope of a Middle Triassic carbonate platform: The Latermar (Dolomites, Italy). Facies, 50, 573-614.

Famin, V., Michon, L., 2010. Volcano destabilization by magma injections in a detachment. Geology, 38, 219-222.

Faure, M., Ishida, K., 1990. The Mid-Upper Jurassic olistostrome of the west Philippines: a distinctive key-marker for the North Palawan block. Journal of Southeast Asian Earth Sciences, 4, 61-67.

Fiduk, J.C., Brush, E.R., Anderson, L.E., Gibbs, P.B., Rowan, M.G., 2004. Salt deformation, magmatism, and hydrocarbon prospectivity in the Espirito Santo Basin, offshore Brazil. In: Post, P.J., Olson, D., Lyons, K.T., Palmes, S.L., Harison, P.F., Rosen, N.C. (eds). Salt-sediment interactions and hydrocarbon prospectivity: Concepts, applications, and case studies for the 21st century. GCSSEPM 24th Annual Conference, p. 370-392.

Fortuin, A.R., 1977. Stratigraphy and sedimentary history of the Neogene deposits in the Ierapetra region, Eastern Crete. GUA papers in Geology, 8, 1-164.

Fortuin, A.R., 1978. Late Cenozoic history of eastern Crete and implications for the geology and geodynamics of the southern Aegean region. Geologie Mijnbouw, 57, 451-464.

Fortuin, A.R., Krijgsman, W., 2003. The Messinian of the Nijar Basin (SE Spain): sedimentation, depositional environments and paleogeographic evolution. Sedimentary Geology, 160, 213–242.

Fortuin, A.R., Peters, W., 1984. The Prina Complex in eastern Crete and its relationship to possible Miocene strike-slip tectonics. Journal of Structural Geology, 6, 459-476.

Fossen, H., 2010. Structural Geology, Cambridge University Press, Cambridge, 480 pp.

França, R. L., del Rey, A. C., Tagliari, C. V., Brandão, J. R., Fontanelli, P.R. 2007, Bacia do Espírito Santo. Boletim Geociências da Petrobras, 15, 501-509.

Frey-Martinez, J., Cartwright, J., James, D., 2006. Frontally confined versus frontally emergent submarine slides: A 3D seismic characterisation. Marine and Petroleum Geology, 23, 585-604.

Gamboa, D. Alves, T., Cartwright, J., 2011. Distribution and characterization of failed (mega) blocks along salt ridges, southeast Brazil: Implications for vertical fluid flow on continental margins. Journal of Geophysical Research: Solid Earth, 116, B8, doi: 10.1029/2011JB008357.

Gamboa, D., Alves, T.M., 2015a. Fault meshes and multi-layered shearing of blocks controlling fluid flow on continental margins. Tectonophysics, 647-648, 21–32.

Gamboa, D., Alves, T.M., 2015b. Spatial and dimensional relationships of submarine slope architectural elements: a seismic-scale analysis from the Espírito Santo Basin, SE Brazil. Marine and Petroleum Geology, 64, 43-57.

Gambôa, L.A.P., Buffler, R.T., Barker, P.F., 1983. Seismic stratigraphy and geologic history of the Rio Grande Gap and southern Brazil basin. Init. Rep. DSDP 72, pp. 481–498.

Gapais, D., 1989. Shear structures within deformed granites: Mechanical and thermal indicators. Geology, 17, 1144-1147.

Garcia, M., Hérail, G., 2005. Fault-related folding, drainage network evolution and valley incision during the Neogene in the Andean Precordillera of Northern Chile. Geomorphology, 65, 279-300.

Garrett, R.G., Thorleifson, L.H., 1999. The provenance of Prairie tills and its importance in mineral exploration. *In*: Ashton, K.E. and Harper, C.T. (ed), Advances in Saskatchewan Geology and Mineral Exploration. Saskatchewan Geological Society, Special Publication, 14, 155-162.

Gawthorpe, R.L., Clemney, H., 1985. Geometry of submarine slides in the Bowland Basin (Dinantian) and their relation to debris flows. Journal of the Geological Society, 142, 555-565.

Gee, M.J.R., Gawthorpe, R.L., Friedmann, J.S., 2005. Giant striations at the base of a submarine slide. Marine Geology, 214, 287–294.

Goff, J., Nichol, S., Kennedy, D., 2010. Development of a palaeotsunami database for New Zealand. Natural Hazards, 54, 193-208.

Graziano, R., 2001. The Cretaceous megabreccias of the Gargano Promontory (Apulia, southern Italy): their stratigraphic and genetic meaning in the evolutionary framework of the Apulia Carbonate Platform. Terra Nova, 13, 110-116.

Gregory-Wodzicki, K.M., 2000. Uplift history of the Central and Northern Andes: A review. Geological Society of America Bulletin, 112, 1091-1105.

Gutscher, M.-A., Dominguez, S., Westbrook, G.K., Gente, P., Babonneau, N., Mulder, T., Gonthier, El., Bartolome, R., Luis, J., Rosas, F., Terrinha, P. and the The Delila and DelSis Scientific Teams, 2009. Tectonic shortening and gravitational spreading in the Gulf of Cadiz accretionary wedge: Observations from multi-beam bathymetry and seismic profiling. Marine and Petroleum Geology, 26, 647-659.

Haflidason, H., Sejrup, H.P., Nygard, A., Mienert, J., Bryn, P., Lien, R., Forsberg, C.F., Berg, K., Masson, D., 2004. The Storegga Slide: architecture, geometry and slide development. Marine Geology, 213, 201-234

Hampton, M.A., Lee, H.J., Locat, J., 1998. Submarine Slides. Reviews of Geophysics, 34, 33-59.

Harbitz, C.B., Glimsdal, S., Bazin, S., Zamora, N., Løvholt, F., Bungum, H., Smebye, H., Gauer, P., Kjekstad, O., 2012. Tsunami hazard in the Caribbean: Regional exposure derived from credible worst case scenarios. Continental Shelf Research, 38, 1-23.

Haughton, P.D.W. 1994. Deposits of deflected and ponded turbidity currents, Sorbas Basin, southeastern Spain: Journal of Sedimentary Research, A64, 223–246.

Haughton, P.D.W., 2000. Evolving turbidite systems on a deforming basin floor, Tabernas, SE Spain. Sedimentology, 47, 497–518.

Hiscott, R.N., James, N.P., 1985. Carbonate debris flows, Cow Head Group, Western Newfoundland. Journal of Sedimentary Petrology, 55, 735-745.

Hodgson, D.M., Haughton, P.D.W., 2004. Impact of syndepositional faulting on gravity current behaviour and deep-water stratigraphy: Tabernas-Sorbas Basin, SE Spain. In: Lomas, S.A. and

Joseph, P. (eds), Confined Turbidite Systems. Geological Society, London, Special Publications, 222, 135-158.

Hühnerbach, V., Masson, D.G., 2004. Slides in the North Atlantic and its adjacent seas: an analysis of their morphology, setting and behaviour. Marine Geology, 213, 343-362.

Idárraga-García, J., Vargas, C.A., 2014. Morphological expression of submarine slides in the accretionary prism of the Caribbean continental margin of Colombia. In: Krastel, S. et al. (eds.) Submarine Mass Movements and Their Consequences, Advances in Natural and Technological Hazards Research, 37, DOI 10.1007/978-3-319-00972-8 35.

Ilstad, T., De Blasio, F., Elverhøi, A., Harbitz, C.B., Engvik, L., Longva, O., Marr, J.G., 2004. On the frontal dynamics and morphology of submarine debris flows. Marine Geology, 213, 481-497.

James, N.P., 1981. Blocks of calcified algae in the Cow Head Breccia, western Newfoundland: Vestiges of a Cambro-Ordovician platform margin. Geological Society of America Bulletin, 92, 799-811.

Jackson, C. A-L, 2011. Three-dimensional seismic analysis of megaclast deformation within a mass transport deposit; implications for debris flow kinematics. Geology, 39, 203-206.

Jackson, M.P.A., Vendeville, B.C., 1994. Regional extension as a geological trigger for diapirism. Geological Society of America Bulletin, 106, 57-73.

Jenner, K.A., Piper, D.J.W., Campbell, D.C., Mosher, D.C., 2007. Lithofacies and origin of late Quaternary mass transport deposits in submarine canyons, central Scotian Slope, Canada. Sedimentology, 54, 19-38.

Jo, A., Eberli, G.P., Grasmueck, M., 2015. Margin collapse and slope failure along southwestern Great Bahama Bank. Sedimentary Geology, 317, 43-52.

Kerckhove, C., 1964. Mise en évidence d'une série à caractère d'olistostrome au sommet des grès d'Annot (Nummulitique autochtone) sur le pourtour des nappes de l'Ubaye (Alpes franco-italiennes). C. R. Acad. Sci. Paris 259, 4742–4745.

Kerckhove, C., 1969. La Zone du Flysch dans les nappes de l'Embrunais-Ubaye (Alpes occidentales). Géologie Alpine, Grenoble 45, 5–204.

Kerckhove, C., 1974. Notice explicative de la Carte géologique de France au 1/50000, feuille Barcelonnette (895). Bur. Rech. Géol. Min. Orléans.

Kleverlaan, K. (1987) Gordo megabed: a possible seismite in a Tortonian submarine fan, Tabernas basin, Province Almeria, southeast Spain. Sed. Geol., 51(3-4), 165-180.

Kleverlaan, K., 1989a. Three distinctive feeder-lobe systems within one time slice of the Tortonian Tabernas fan, SE Spain. Sedimentology, 36, 25-45.

Kleverlaan, K., 1989b. Neogene history of the Tabernas basin (SE Spain) and its Tortonian submarine fan development. Geologie Mijnbouw, 68, 421-432.

Kumar, N., Gambôa, L.A.P., Schreiber, B.C. et al., 1997. Geologic history and origin of Sao Paulo Plateau (southeastern Brazilian margin), comparison with the Angolan margin and the early evolution of northern South Atlantic, *In*: Supko, P. R., Perch-Nielsen, K., andothers, Initial reports of the Deep Sea Drilling Project, Vol. 39: Washington, D.C., U.S. Government Printing Office, p. 927 -945.

Kvalstad, T.J., Andresen, L., Forsberg, C.F., Berg, K., Bryn, P., Wangen, M., 2005. The Storegga Slide: Evaluation of triggering sources and slide mechanics. Marine and Petroleum Geology, 22 , 245-256.

Labazuy, P., 1996. Recurrent slides events on the submarine flank of Piton de la Fournaise volcano (Reunion Island). Journal of the Geological Society, London,110, 295-306.

Laberg, J.S., Vorren, T.O., 2005. Flow behaviour of the submarine glacigenic debris flows on the Bear Island through Mouth Fan, western Barents Sea. Sedimentology, 47, 1104-1117.

Lamarche, G., Joanne, C., Collot, J.-Y., 2008. Successive, Large Mass-Transport Deposits in the South Kermadec Fore-Arc Basin, New Zealand: the Matakaoa Submarine Instability Complex. Geochemistry, Geophysics, Geosystems. 9, Q04001.

Lénat, J.F., Bachelery, P., Bonneville, A., Tarits, P., Cheminee, J.L., Delorme, H., 1989. The December 1983-January 1984 eruption of Piton de la Fournaise volcano, Reunion Island. Journal of Volcanology and Geothermal Research, 36, 87-112.

Lénat, J.F., Bachelery, P., Merle, O., 2012. Anatomy of Piton de la Fournaise volcano (La Réunion, Indian Ocean). Bulletin of Volcanology, 74, 1945-1961.

Leslie, S.C., Moore, G.F., Morgan, J.K., Hills, D.J., 2002. Seismic stratigraphy of the Frontal Hawaiian Moat: implications for sedimentary processes at the leading edge of an oceanic hotspot trace. Marine Geology, 184, 143-162.

Lipman, P.W., Eakins, B.W., Yokose, H., 2003. Ups and downs on spreading flanks of ocean-island volcanoes: Evidence from Mauna Loa and Kīlauea. Geology, 31, 841-844.

Lourenço, S., Sassa, K., Fukuoka, H., 2006. Failure process and hydrologic response of a two layer physical model: Implications for rainfall-induced landslides. Geomorphology, 73, 115-130.

Lucente, C.C., Pini. G.A., 2003. Anatomy and emplacement mechanism of a large submarine slide within a Miocene foredeep in the northern Apennines, Italy: A field perspective. American Journal of Science, 303, 565-602.

Mandl, G., 2000. Fault structures. In: G. Mandl (ed), Faulting in Brittle Rocks: An Introduction to the Mechanics of Tectonic Faults, Springer-Verlag, Berlin, pp. 215-297.

Martín, J.M., Braga, J.C., 1994. Messinian events in the Sorbas Basin in southeastern Spain and their implications in the recent history of the Mediterranean. Sedimentary Geology, 90. 257-268.

Martinsen, O.J., Bakken, B., 1990. Extensional and compressional zones in slumps and slides in the Namurian of County Clare, Ireland. Journal of the Geological Society of London, 147, 153-164.

Martinsen, O., 1994. Mass movements. In: Maltman, A. (ed.), The Geological Deformation of Sediments. Chapman & Hall, London, p. 127-165.

Masson, D. G. 1996 Catastrophic collapse of the flank of El Hierro about 15,000 years ago, and the history of large flank collapses in the Canary islands. Geology, 24, 231–234.

Masson, D.G., Watts, A.B., Gee, M.J.R., Urgeles, R., Mitchell, N.C., Le Bas, T.P., Canals, M., 2002. Slope failures on the flanks of the western Canary Islands. Earth-Science Reviews, 57, 1-35.

Masson, D.G., Harbitz, C.B., Wynn, R.B., Pedersen, G., Løvholt, 2006. Submarine slides: processes, triggers and hazard prediction. Philosophical Transactions of the Royal Society A, 1845, 2009-2039.

Master, S., Rainauld, C., Armstrong, R.A., Phillips, D., Robb, L.J., 2005. Provenance ages of the Neoproterozoic Katanga Supergroup (Central African Copperbelt), with implications for basin evolution. Journal of African Earth Sciences, 42, 41-60.

Master, S., Wendorff, M., 2011. Chapter 12 - Neoproterozoic glaciogenic diamictites of the Katanga Supergroup, Central Africa. Geological Society, London, Memoirs, 36, p. 173-184.

Matsuda, S., Ogawa, Y., 1993. Two-stage model of incorporation of seamount and oceanic blocks into sedimentary melange: Geochemical and biostratigraphic constraints in Jurassic Chichibu accretionary complex, Shikoku, Japan. Island Arc, 2, 7-14.

Mauduit, T., Guérin, G., Brun, J.-P., Lecanu, H., 1997. Raft tectonics: the effects of basal slope angle and sedimentation rate on progressive extension. Tectonophysics, 19, 1219-1230.

McGuire, W.J., 2003. Volcano instability and lateral collapse. Revista, I, 33-45.

Mehl, K.W., Schmincke, H.-U., 1999. Structure and emplacement of the Pliocene Roque Nublo debris avalanche deposit, Gran Canaria, Spain. Journal of Volcanology and Geothermal Research, 94, 105-134.

Meisling, K.E., Cobbold, P.R., Mount, V.S., 2001. Segmentation of an obliquely rifted margin, Campos and Santos basins, southeastern Brazil. American Association of Petroleum Geologists Bulletin, 85, 1903-1924.

Micallef, A., Masson, D.G., Berdnt, Ch., Stow, D.A.V., 2007. Morphology and mechanics of submarine spreading: A case study from the Storegga Slide. Journal of Geophysical Research: Earth Surface, 112, doi: 10.1029/2006JF000739.

Mills, P.C., 1983. Genesis and diagnostic value of soft-sediment deformation structures - A review. Sedimentary Geology, 35, 83-104.

Migeon, S., Cattaneo, A., Hassoun, V., Larroque, Ch., Corradi, N., Fanucci, F., Dano, A., Mercier de Leinay, B., Sage, F., Gorini, Ch., 2011. Morphology, distribution and origin of recent submarine slides of the Ligurian Margin (North-western Mediterranean): some insights into geohazard assessment. Marine Geophysical Researches, 32, 225-243.

Moore, G.F., et al., 2009, Structural and seismic stratigraphic framework of the NanTroSEIZE State 1 transect, in NanTroSEIZE Stage 1: Investigations of Seismogenesis, Nankai Trough, Japan: Proceedings Integrated Ocean Drilling Program 314/315/316, doi:10.2204/iodp.proc.314315316.102.2009.

Moore, J.G., Bryan, W.B., Beeson, M.H., Normark, W.R., 1995. Giant blocks in the South Kona slide, Hawaii. Geology, 23, 125-128.

Moore, J.G., Chadwick Jr., W.W., 1995. Offshore geology of Mauna Loa and adjacent areas, Hawaii. Geophysical Monograph 02, American Geophysical Union, 21-44.

Morris, A.P., Ferrill, D.A., Henderson, D.B., 1996. Slip tendency analysis and fault reactivation. Geology 24, 275-278.

Moscardelli, L., Wood, L. J., Mann, P., 2006. Mass-transport complexes and associated processes in the offshore area of Trinidad and Venezuela. American Association of Petroleum Geologists Bulletin, 90, 7, 1059–1088.

Nemec, W., 1990. Aspects of sediment movement on steep delta slopes. Special publication of the International Association of Sedimentologists, 10, 20-73.

Nichols, R.J., 1995. The liquification and remobilization of sandy sediments. In: Hartley, A.J., Prosser, D.J. (eds.), Characterization of Deep Marine Clastic Systems, Special Publications, Geological Society, London, 94, pp. 63–76.

Ogata, K., Pogačnik, Ž., Pini, G.A., Tunis, G., Festa, A., Camerlenghi, A., Rebesco, M., 2014. The carbonate mass transport deposits of the Paleogene Friuli Basin (Italy/Slovenia): internal anatomy and inferred genetic processes. Marine Geology, 356, 88–110.

Ogiesoba, O., Hammes, U., 2012. Seismic interpretation of mass-transport deposits within the upper Oligocene Frio Formation, south Texas Gulf Coast. American Association of Petroleum Geologists Bulletin, 96, 845– 868.

Omosanya, K.O., Alves, T.M., 2013. Ramps and flats of mass-transport deposits (MTDs) as markers of seafloor strain on the flanks of rising diapirs (Espírito Santo Basin, SE Brazil). Marine Geology, 340, 82-97.

Owen, G., 1987. Deformation processes in unconsolidated sands ,in: M.E. Jones, R.M.F. Preston (Eds.), Special Publications, Geological Society, London, 29, 11–24.

Pêcher, A., Baférty, J.C., Gidon, M., 1992. Structures est-ouest anténummulitiques à la bordure orientale du massif des Encrins-Pelvoux (Alpes francaises). In: Dumont, T.; Mascle, G.; Tricart, Géologie alpine. Serie spéciale; Colloques et excursions, ISSN 1247-0236.

Penge, J.,Munns, J.W.,Taylor, B.,Windle, T.M.F., 1999. Rift-raft tectonics: examples of gravitational tectonics from the Zechstein basins on northwest Europe. In: Fleet, A.J., Boldy, S.A.R. (Eds.), Petroleum Geology of Northwest Europe, Proceedings of the 5th Conference, pp. 201-213.

Perotti, E., Bertok, C., d'Atri, S., Martire, L., Piana, F., Catanzariti, R., 2012. A tectonically-induced Eocene sedimentary mélange in the West Ligurian Alps, Italy. Tectonophysics, 568-569, 200-214.

Pilcher, R.S., Murphy, R.T., Ciosek, J.M., 2014. Jurassic raft tectonics in the northeastern Gulf of Mexico. Interpretation, 2, SM39-SM55.

Platt, J.P., Vissers, R.L.M., 1980. Extensional structures in anisotropic rocks. Journal of Structural Geology 2 (4), 397–410.

Pohler, S.M.L., James, N.P., 1989. Reconstruction of a Lower/Middle Ordovician Carbonate Shelf margin: Cow Head Group, Western Newfoundland. Facies, 21, 189-262.

Posamentier, H.W., Kolla, V., 2003. Seismic geomorphology and stratigraphy of depositional elements in deep-water settings. Journal of Sedimentary Research, 73, 367–388.

Postma, G., Drinia, H., 1993. Architecture and sedimentary facies evolution of a marine, expanding outer-arc half-graben (Crete, late Miocene). Basin Research, 5, 103-124.

Postma, G., Fortuin, A.R., van Wamel, W.A., 1993. Basin-fill patterns controlled by tectonics and climate: the Neogene 'fore-arc' basins of eastern Crete as a case history. In: Frostick, L.E., Steel, R.J. (eds), Tectonic Controls and Signatures in Sedimentary Successions. International Association of Sedimentologists, Special Publications, 20, 335-362.

Powrie, W., 2002. Soil Mechanics, Concepts and Applications, Spon Press.

Principaud, M., Mulder, T., Gillet, H., Borgomano, J., 2015. Large-scale carbonate submarine mass-wasting along the northwestern slope of the Great Bahama Bank (Bahamas): Morphology, architecture, and mechanisms. Sedimentary Geology, 317, 27-42.

Quirk, D.G., Schødt, N., Lassen, B., Ings, S.J., Hsu, D., Hirsch, K.K., Von Nicolai, Ch., 2012. Salt tectonics on passive margins: examples from Santos, Campos and Kwanza basins. Geological Society London, Special Publications, 363, 207-244.

Rees, B.A., Detrick, R.S., Coakley, B.J., 1993. Seismic stratigraphy of the Hawaiian flexural moat. Bulletin of the Geological Society of America,105, 189-205.

Roep, T.B., Fortuin, A.R., 1996. A submarine slide scar and channel filled with slide blocks and megarippled Globigerina sands of possible contourite origin from the Pliocene of Sumba, Indonesia. Sedimentary Geology, 103, 145-160.

Rouby, D., Raillard, S., Guillocheau, F., Bouroullec, R., Nalpas, T., 2002, Kinematics of a growth fault/raft system on the West African margin using 3-D restoration. Journal of Structural Geology, 24, 783-796.

Saint-Ange, F., Bachelery, P., Babonneau, N., Michon, L., Jorry, S., 2013. Volcaniclastic sedimentation on the submarine slopes of a basaltic hotspot volcano: Piton de la Fournaise volcano (La Réunion Island, Indian Ocean). Marine Geology, 337, 35-52.

Sen, K., Das, S., Mukherjee, B.K., Sen, K., 2013. Bimodal stable isotope signatures of Zildat Ophiolitic Mélange, Indus Suture Zone, Himalaya: implications for emplacement of an ophiolitic mélange in a convergent setup. International Journal of Earth Sciences, 102, 2033-2042.

Shibakova, V.S., Grigorieva, S.V., Korobanova, I.C., 1977. Clayey zones in a rock massif and their role in slide development. Bulletin of Engineering Geology and the Environment, 16, 233–235.

Shu, L., Wang, B., Zhu, W., Guo, Z., Charvet, J., Zhang, Y., 2011. Timing of initiation of extension in the Tianshan, based on structural, geochemical and geochronological analyses of bimodal volcanism and olistostrome in the Bogda Shan (NW China). International Journal of Earth Sciences, 100, 1647-1663.

Shuzui, H., 2001. Process of slip surface development and formation of slip-surface clay in slides in Tertiary volcanic rocks, Japan. Engineering Geology, 61, 199-219.

Siebert, L., 1984. Large volcanic debris avalanches: characteristics of source areas, deposits, and associated eruptions. Journal of Volcanology and Geothermal Research, 22, 163–197.

Soares, D.M., Alves, T.M. and Terrinha, P., 2014. Contourite drifts on distal margins as indicators of established lithospheric breakup. Earth and Planetary Science Letters, 401, 116-131. (10.1016/j.epsl.2014.06.001)

Solheim, A., Bryn, P., Sejrup, H.P., Mienert, J., and Berg, K., 2005. Ormen Lange-an integrated study for the safe development of a deep-water gas field within the Storegga Slide Complex, NE Atlantic continental margin; executive summary. Marine and Petroleum Geology, 22, 1-9.

Spence, G.H., Tucker, M.E., 1997. Genesis of limestone megabreccias and their significance in carbonate sequence stratigraphic models: a review. Sedimentary Geology, 112, 163-193.

Strasser, M., Moore, G.F., Kimura, G., Kopf, A.J., Underwood, M.B., Guo, J., Screaton, J., 2011. Slumping and mass transport deposition in the Nankai fore arc: Evidence from IODP drilling and

3-D reflection seismic data. Geochemistry, Geophysics, Geosystems, 12, doi: 10.1029/2010GC003431.

Talling, P.J., Wynn, R.B., Masson, D.G., Frenz, M., Cronin, B.T., Schiebel, R., Akhmetzhanov, A.M., Dallmeier-Tiessen, S., Benetti, S., Weaver, P.P.E., Georgiopoulou, A., Zühlsdorff, C., Amy, L.A., 2007. Onset of submarine debris flow deposition far from original giant slide. Nature, 450, 541-544.

Ten Veen, J. H. and Postma G., 1999a. Neogene tectonics and basin fill patterns in the Hellenic outer-arc (Crete, Greece). Basin Research, 11, 223-242.

Ten Veen, J. H. and Postma G., 1999b. Roll-back controlled vertical movements of outer-arc basins of the Hellenic subduction zone (Crete, Greece). Basin Research, 11, 243-267.

Tikoff, B., Greene, D., 1997. Stretching lineations in transpressional shear zones: an example from the Sierra Nevada Batholith, California. Journal of Structural Geology, 19, 29-39.

Trincardi, F., Normark W.R., 1989. Pleistocene Suvero slide, Paola basin, southern Italy. Marine and Petroleum Geology, 6, 324-335.

Trincardi, F., Argnami, A., 1990. Gela Submarine slide: a major basin-wide event in the Plio-Quatemary foredeep of Sicily. Geo-Marine Letters, 10, 13-21.

Trofimovs, J., Davis, B.K., Cas, R.A.F., 2004, Contemporaneous ultramafic and felsic intrusive and extrusive magmatism in the Archaean Boorara Domain, Eastern Goldfields Superterrane, Western Australia, and its implications: Precambrian Research, v. 131, pp. 283–304.

van Hinsbergen, D.J.J., Meulenkamp, J.E., 2006. Neogene supradetachment basin development on Crete (Greece) during exhumation of the South Aegean core complex. Basin Research, 18, 103-124.

Varnes, D. J. 1978. Slope movement types and processes. In: Special Report 176: Slides: Analysis and Control (Eds: Schuster, R. L. & Krizek, R. J.). Transportation and Road Research Board, National Academy of Science, Washington D. C., 11-33.

Viana, A., Figueiredo, A., Faugeres, J.-C., Lima, A., Gonthier, E., Brehme, I., Zaragosi, S., 2003. The Sao Tomé deep-sea turbidite system (southern Brazil Basin): Cenozoic seismic stratigraphy and sedimentary processes. AAPG Bulletin, 87, 873-894.

Watts, A.B., Masson, D.G., 2001. New sonar evidence for recent catastrophic collapses of the north flank of Tenerife, Canary Islands. Bulletin of Volcanology, 63, 8-19.

Wendorff, M., 2000. Genetic aspects of the Katangan megabreccias: Neoproterozoic of Central Africa. Journal of African Earth Sciences, 30, 703-715.

Wendorff, M., 2001. New exploration criteria for 'megabreccia'-hosted Cu-Co deposits in the Katangan belt, central Africa, In: Piestrzynski, A. et al. (eds.), Mineral Deposits at the Beginning of the 21st Century. Swets & Zeitlinger Publishers, Lisse, Netherlands, pp. 19-22

Wendorff, M., 2003. Stratigraphy of the Fungurume Group - evolving foreland basin succession in the Lufilian fold-thrust belt, Neoproterozoic-Lower Palaeozoic, Democratic Republic of Congo. South African Journal of Geology, 106, 17-34.

Wendorff, M., 2005a. Evolution of Neoproterozoic–Lower Palaeozoic Lufilian arc, Central Africa: a new model based on syntectonic conglomerates. Journal of the Geological Society, London, 162, 5-8.

Wendorff, M., 2005b. Sedimentary genesis and lithostratigraphy of Neoproterozoic megabreccia from Mufulira, Copperbelt of Zambia. Journal of African Earth Sciences, 42, 61-81.

Wendorff, M., 2011. Tectonosedimentary expressions of the evolution of the Fungurume foreland basin in the Lufilian Arc, Neoproterozoic–Lower Palaeozoic, Central Africa. Journal of the Geological Society, London, 357, 69-83.

White, S.H., 1979. Large strain deformation: report on a Tectonic Studies Group discussion meeting held at Imperial College, London on 14 November 1979. Journal of Structural Geology, 1, 333–339.

Wolfe, C.J., McNutt, M.K., Detrick, R.S., 1994. The Marquesas archipelagic apron: seismic stratigraphy and implications for volcano growth, mass wasting, and crustal underplating. Journal of Geophysical Research, 99, 13,591-13,608.

Yokose, H., Lipman, P.W., 2004. Emplacement mechanisms of the South Kona slide complex, Hawaii Island: Sampling and observations by remotely operated vehicle Kaiko. Bulletin of Volcanology, 66, 569-584.

Figure Captions

Figure 1 - Location map of the studied 3D seismic volumes and outcrop locations referred to in this paper. Outcrop areas in SE Crete and SE Spain are indicated in bold.

Figure 2 - Location maps of the 3D seismic profiles interpreted in this work. (a) Location of seismic profiles in the pre-stack time migrated (PSTM) seismic volume from the Espírito Santo Basin, SE Brazil. Modified from Alves (2010). (b) Location of Fig. 7d in the PSDM seismic volume from the Nankai Trough (from Alves et al., 2014c). (c) Location of the seismic line shown in Fig. 6a, imaging a faulted MTD from SE Brazil (Espírito Santo Basin). Modified from Alves et al. (2014b). See Fig. 1 for the location of the 3D seismic volumes in this work.

Figure 3 – (a) Inset showing the location of the investigated slope successions in SE Crete. (b) Geological map of the Ierapetra paleoslope. Area 1 on the geological map comprises autochthonous carbonate blocks and breccia–conglomerates denoting limited gravitational collapse. Area 2 comprises disrupted deep-water (carbonate) fan cones, carbonate megabreccias and boulder conglomerates. Area 3 includes carbonate fan cones, collapsed blocks, and minor debris-flow deposits (boulder conglomerates) deposited in distal regions of the Ierapetra

paleoslope. Geological map was modified from Alves and Lourenço (2010). (c) Stratigraphic units from the Ierapetra Basin, SE Crete, a tectonic trough subject to transtensive movements since, at least, the end of the Serravalian (from Postma and Drinia, 1993 and van Hinsbergen et al., 2006). SP-Stratified Prina Series.

Figure 4 – Examples of blocks referred to in this paper. (a) Detail of the lithological character of the 'schiste à blocs' unit from the western Alps, SE France. The 'schiste à blocs' were deposited adjacently to a W- and SW-moving series of thrusted alpine nappes, exhumed and eroded in the Paleogene (Dummont et al., 2011). (b) Rafted block from the Ierapetra paleoslope, SE Crete. The imaged block is 140-m high and is interbedded with marine sands and clays of Tortonian age (Fortuin, 1977; Alves and Lourenço, 2010). (c) Blocks from the glaciated margin of Labrador, suggestively triggered by local earthquakes. The width of blocks in this example reach more than 1 km for a heights exceeding 500 ms (200-300 m; Deptuck et al., 2007). (d) Detail of rafted blocks from West Iberia generated during continental breakup (Soares et al., 2014). Top BS refers to the top of a *breakup sequence* as defined by the latter authors. LBS refers to *Lithospheric Breakup Surface* as defined by Soares et al. (2014).

Figure 5 – Examples of blocks on seismic data: (a) Miocene blocks from the Espírito Santo Basin forming large (>400-m thick) collapse features. Modified from Alves (2010). (b) Blocks from the Santos Basin as interpreted in Jackson (2010) for SE Brazil. Blocks were seen in this case as deforming despite being cohesive and the flow in which they were lacked turbulence. (c) Blocks from the SE Brazil Espírito Santo Basin, imaged as coherent volumes of strata imbedded in debrites and turbidites, some of them remnant in nature. See Gamboa et al. (2011) for more information. (d) Coherency map depicting the areal distribution of blocks over the same salt structure shown in (c). Note the preferential distribution of blocks towards the fringes of the diapirs' flanks.

Figure 6 – (a) Seismic profile from SE Brazil showing the geometry of differential compaction features above, and over the flanks of Miocene blocks (see Alves, 2010 for more information). (b) Time-structure map showing the orientation and geometry of depressions shown in (a). (c) TWT depth of depressions in the same region of the Espírito Santo Basin. (d) Width vs. length values for depressions in Espírito Santo. Note the average depth of 33 ms for the interpreted depressions, and the established scale relationship between the width and length of these same features.

Figure 7 – Detail of lateral ramps within a blocky MTD from SE Brazil (see Alves et al., 2010). The lateral ramps in this case show sheared and fractured blocks that reflect important strike-slip stresses. (b) Seismic line showing headwall erosion across diachronous strata in the Nankai Trough, SE Japan and the flat-ramp geometry of the basal glide plane. The top of MTD 6 coincides with the blue horizon. The yellow horizon marks the basal glide plane. (c) Time-structure map showing the geometry of crown scarps (s) and ramps from the same MTD in SE Japan (MTD 6 in Alves et al., 2014b).

Figure 8 – (a) Detail of a basal glide plane from SE Brazil revealing distinct thickness and structural deformation on seismic data. Note the transparent region of ~50 ms that separates the rotated blocks from the continuous surface usually mapped as the basal glide plane. This basal glide plane is highly deformed. (b) Detail of ramp-bounded promontories formed around salt diapirs in SE Brazil (see Omosanya and Alves, 2013).

Figure 9 – Example of internal deformation in submarine slide blocks from SE Brazil (see Gamboa and Alves, 2015a). In this seismic section are observed a series of small-scale thrusts indicating late collapse (and intra-bed movement) of individual blocks.

Figure 10 – Field photographs highlighting the remobilization styles of MTDs observed on the Ierapetra paleoslope, SE Crete. (a) Autochthonous carbonate blocks in proximal areas of the Ierapetra paleoslope (Area 1 in Fig. 3b). (b) Sandy blocks embedded in collapsed strata accumulated in intermediate regions of the Ierapetra paleoslope (Area 2 in Figure 3b). (c) Megabreccias marking the base of the Prina Complex at Ierapetra, and the onset slope instability in SE Crete's Tortonian margin. (d) Detail of carbonate fan cones and debris flows deposited at the base of the Ierapetra paleoslope, close to Mirtos (Fig. 3b). (e) Erosional contact at the base of block in Ierapetra. (f) Rotation slides at Agios Dimitrios, location 22, on the Ierapetra paleoslope. (g) Chasms in collapsed blocks outcropping in at the base of the Ierapetra paleoslope. (h) Glide plane structures in a block transported from Area 1 to the toe of the Ierapetra paleoslope (Area 3, Fig. 3b).

Figure 11 – Detailed photos of soft-sediment kinematic indicators recorded in SE Crete. (a) Foliation in shales in the basal glide plane of a collapsed block. (b) Example of foliated strata and fragmented megabreccia clasts under a collapsed block in location 22. (c) Pull-apart structures in interbedded clay-silt intervals deformed below a collapsed block. (d) Dilational jogs and tear faults in strata deformed below the Agios Dimitrios block, location 22. (e) Intrafolial folds observed at the same location as (f) at the base of the Agios Dimitrios blocks. (f) Imbricated and strained clasts in a megabreccia interval present in the same location as the foliation in (a).

Figure 12 – (a) and (b) Aspect of folded successions at the base of the Ierapetra paleoslope, Mirtos-Ierapetra corridor (Fig. 3b). (c) Detail of ramped-up strata (and associated structures) in a Miocene slide from the Tabernas-Sorbas Basin, SE Spain. Note the small-scale thrusts and coarse foliation observed in the MTD just above the basal ramp. (d) Detail of foliation formed at

the toe of the MTD shown in (c), a reliable indicator of local shearing in the direction of transport of the interpreted MTD.

Figure 13 – Retrogressive slide model completed by Kvalstad et al. (2005) for slide blocks in the Storegga Slide. (a) Initial stage of shear-band formation, unloading and surface expansion of strata in blocks. (b) Onset of block movement and strain softening under the weight of displaced overburden capping individual blocks. (c) Acceleration of movement due to progressive strain softening at the base of individual blocks. (d) Complete separation of blocks and generation of shear bands in retrogressive scarps, marking the re-initiation of step (a) in more proximal parts of the slope.

Figure 14 – (a) Detail of the large scale structure of basal glide plane sediments at Agios Dimitrios, Ierapetra paleoslope. (b) Structural features associated with intra-blocks shearing at Agios Dimitrios (location 22). Note the injection of sandy material, mostly liquefied, in the plane separating the two blocks, and the apparent load structures at the base of the uppermost block. (c) 'Flame' structures at a bedding plane separating two large megabreccia beds at Agios Dimitrios (location 22).

Figure 15 – (a) Basal glide plane structure in a large block near Kalamavka, Ierapetra paleoslope (see Fig. 3b). The large thickness of deformed strata at the base of the block results from the loading imposed by this same block when it was transported downslope. (b) Graph showing the scale relationships between the height of outcropping blocks at Ierapetra, and the thickness of the *basal shear zone* below (modified from Alves and Lourenço, 2010). The regression line shows that basal shear zone (BSZ) thickness is ~0.15 of block height.

Figure 16 – Model of block fragmentation and movement in SE Crete, highlighting the structural features formed at specific evolution stages transitional stage. Modified from Gee et al. (2005) and Alves and Lourenço (2010).

Figure 17 – (a) Block from SE Brazil highlighting the internal fault-bounded compartments and chasms depicted in the models shown in (c), (d) and (e). (b) Seismic profile showing the local structure of the modelled blocks. (c) to (e) Panels showing leakage factors modelled for the blocks in (a) and (b). Note that, with changing depths and confining pressures, faults and scarps in the modelled blocks consistently form structures with high leakage factors, as shown by the brighter colours. Darker colours indicate lower values of leakage factor (see Morris et al., 1996).

Table 1 – Summary table of the tectonic settings, ages, lithologies, matrix lithologies and geological significance of submarine slide blocks referred to in this paper.

Table 1

Continent	Country	Tectonic Setting	Age	Megablock Lithologies	Matrix Lithologies	Geological Significance
	Slovenia	Alpine Orogen	Cenozoic	Limestones and dolomites	Siliciclastic units	Erosion of active orogen
	SE Crete	Hellenides Forearc	Late Miocene	Carbonate breccias	Turbidite sands and muds. Marine (proximal) sands.	Uplift of forearc region. Plate convergence with an important strike-slip signature
	NE Italy	Oblique rift margin	Triassic	Dolomitic limestones of reefal environments	Siliciclastic units	Erosion of active rifting margin
	NW Italy	Alpine foreland	Eocene to Oligocene	Polymictic conglomerates	Turbidite muds and sands	Erosion of active foreland thrust-and-fold belt
	SE France	Alpine foreland	Oligocene	Limestones and polymictic conglomerates	Turbidite muds, sands and shales	Exhumation and subsequent emersion of the W Alpine foreland
Europe	N Sicily	Volcanic island group	Pliocene to Quaternary	Basalt blocks	Volcaniclastic sands and conglomerates	Growth and collapse of volcanic islands
	Portugal	Rifted margin	Cretaceous	Unknown	Turbidite sands, muds and black shales	Collapse of fault-bounded continental slope during continental breakup
	S Spain	Plate subduction and transtension	Cenozoic	Turbidite sands and muds	Turbidite sands, muds and evaporites	Convergence between Eurasia and N Africa with uplift of the Atlas
Asia	Indonesia	Plate subduction	Miocene	Sandstones, shales carbonates and basalts	Shales and turbidite muds	Uplift of Sumba due to subduction and associated volcanism
	Australia	Ultramafic Archean volcanism	Archean	Dacite, basalt and komatiite	Dacite, basalt and komatiite with sediment	Collapse of volcanic edifices
Australasia Indian and Pacific Oceans	Hawaii, Marquesas and La Reunion	Oceanic volcanism (hotspots)	Late Cenozoic	Basalt and consolidated volcaniclastic sediment	Volcaniclastic and biogenic sediment	Collapse of volcanic edifices
	New Zealand	Plate subduction	Late Cenozoic	Debrites of sands, consolidated clays and volcaniclastic material	Hemipelagic muds and volcaniclastic material	Erosion of accretionary wedge
	Canada and NE USA	Uplifting Orogen (Appalachians)	Cambrian to Ordovician	Limestone conglomerates, mudstones and grainstones	Qz-rich sandstones, mudstones	Uplift and erosion of a submerged orogen
North and Central America	Canada (Labrador)	Glacial margin subject to earthquake activity	Pliocene-Pleistocene	Hemipelagites and glacial till	Hemipelagites and glacial till	Earthquake triggered landslides on a glacial margin
	Lesser Antilles	Back-arc volcanism	Late Cenozoic	Basalt and consolidated volcaniclastic sediment	Volcaniclastic and biogenic sediment	Collapse of volcanic edifices
	N Colombia	Foreland and strike-slip tectonics	Late Cenozoic	Hemipelagites and deltaic deposits, some consolidated	Finer hemipelagites	Slope oversteepening and earthquakes in major plate boundary
	Bahamas	Passive Margin	Late Cenozoic	Carbonates	Hemipelagites and carbonate ooze	Diagenesis and drift control on basal glide plane
	SE Brazil (Espirito Santo)	Divergent margin with important halokinesis	Eocene	Consolidated volcaniclastic and hemipelagic sediment	Debrites of similar composition	Halokinesis and oversteepening due to Andean tectonics
South America	SE Brazil (Santos Basin)	Divergent margin with important halokinesis	Cenozoic	Consolidated hemipelagites	Debrites of similar composition	Halokinesis and oversteepening due to Andean tectonics
	Argentina Pre-Cordillera	Rimmed carbonate platform	Cambrian-Ordovician	Limestone and dolomites	Sandstones and mudstones	Tectonic oversteepening in orogenic belt
	S Peru	Back-arc basin	Cretaceous	Limestones and dolomites	Hemipelagic muds and sands	Tectonic oversteepening in back-arc basin
	Congo and Zaire	Pan-African Orogen	Pre-Cambrian	Dolomites and limestones. Megabreccias.	Hemipelagic shales and sands	Uplift and erosion of a submerged orogen
Africa	NW Morocco	Atlas Orogen	Late Mesozoic and Cenozoic	Probable limestones and dolomites	Hemipelagic deposits. Turbidites.	Tectonic oversteepening
	Canary Islands	Oceanic volcanism (hotspot)	Cenozoic	Basalt and consolidated volcaniclastic sediment	Volcaniclastic and biogenic sediment	Collapse of volcanic edifices

Table 1

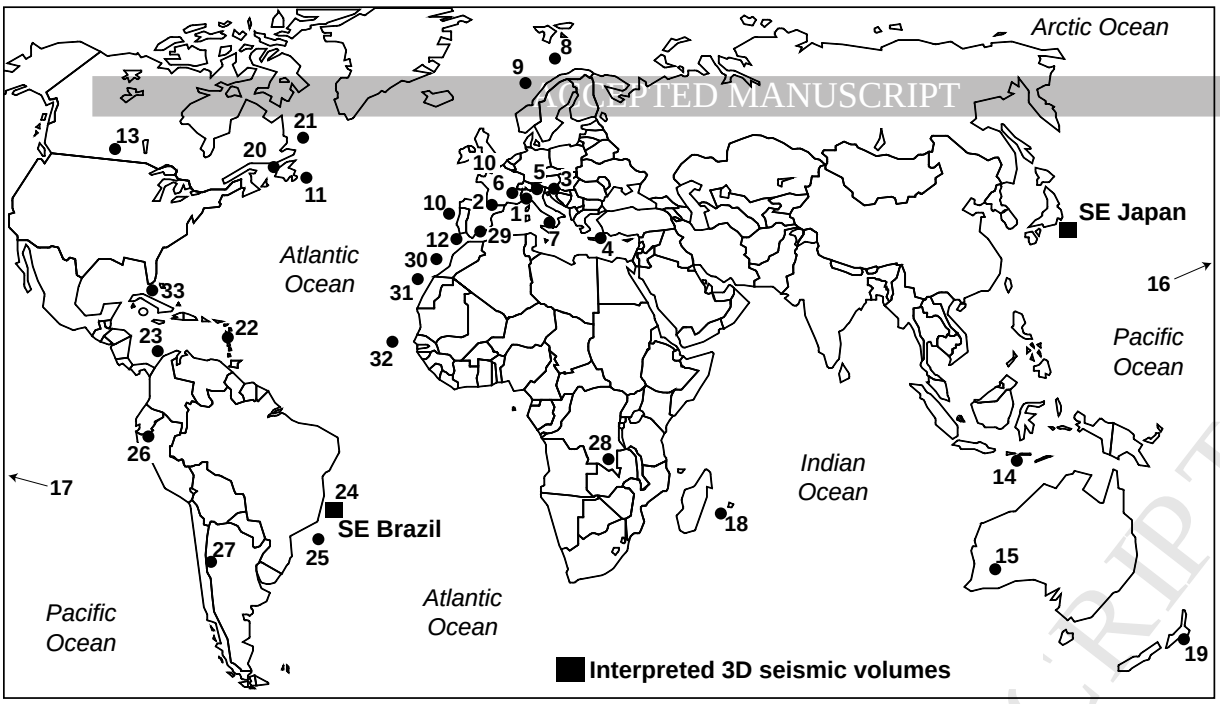

Key locations referred to in this paper

1 - West Liguria (Italy)
2 - Pyrenees
3 - Slovenia and Friuli Basin (Italy)
4 - SE Crete
5 - Italian Dolomites
6 - SE France
7 - Stromboli (Aeolian Islands)
8 - Barents Sea (Norway)
9 - Storegga Slide (Norway)
10 - West Iberia
11 - Newfoundland (E Canada)
12 - SW Iberia
13 - Prairie Region (Canada/USA)
14 - Sumba (Indonesia)
15 - SW Australia
16 - Hawaiian islands
17 - Marquesas Islands
18 - La Reunion
19 - New Zealand
20 - Appalachians (Cow Head Gp.)
21 - Labrador Sea
22 - Lesser Antilles
23 - N Colombia margin
24 - SE Brazil (Espirito Santo)
25 - SE Brazil (Santos Basin)
26 - Peru
27 - Argentina (San Juan)
28 - PanAfrican Orogen (Congo)
29 - Tabernas and Sorbas Basins
30 - W Morocco
31 - Canary islands
32 - Fogo island (Cape Verde)
33 - Great Bahamas Bank

Figure 1 -

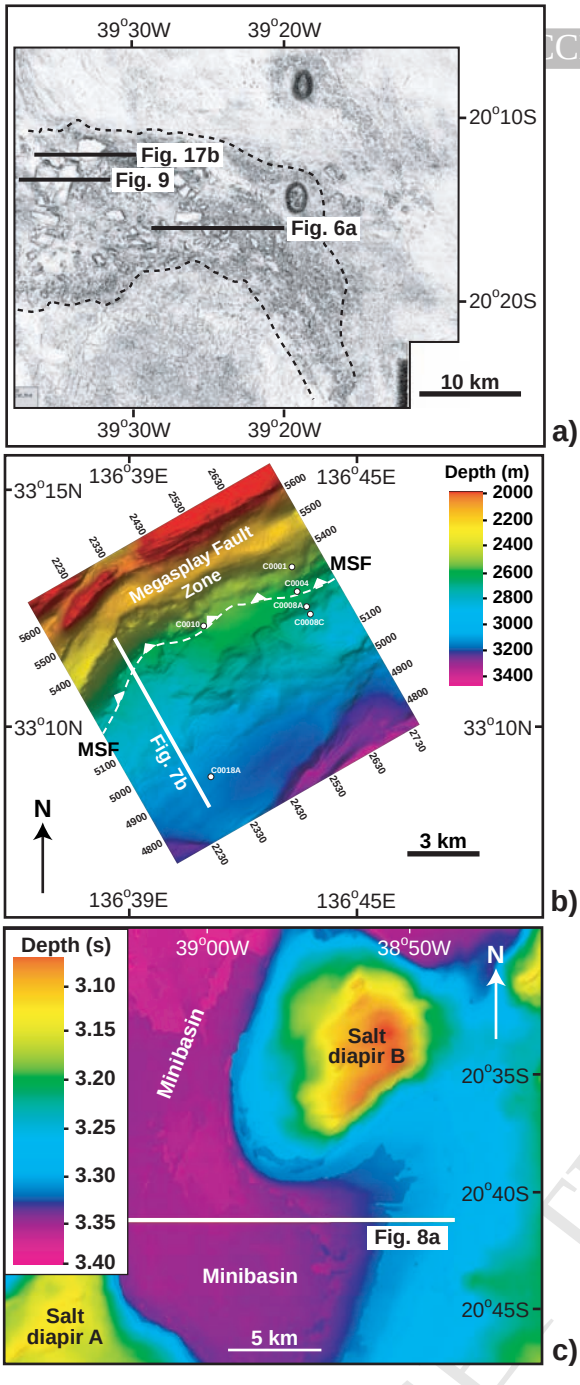

Figure 2 -

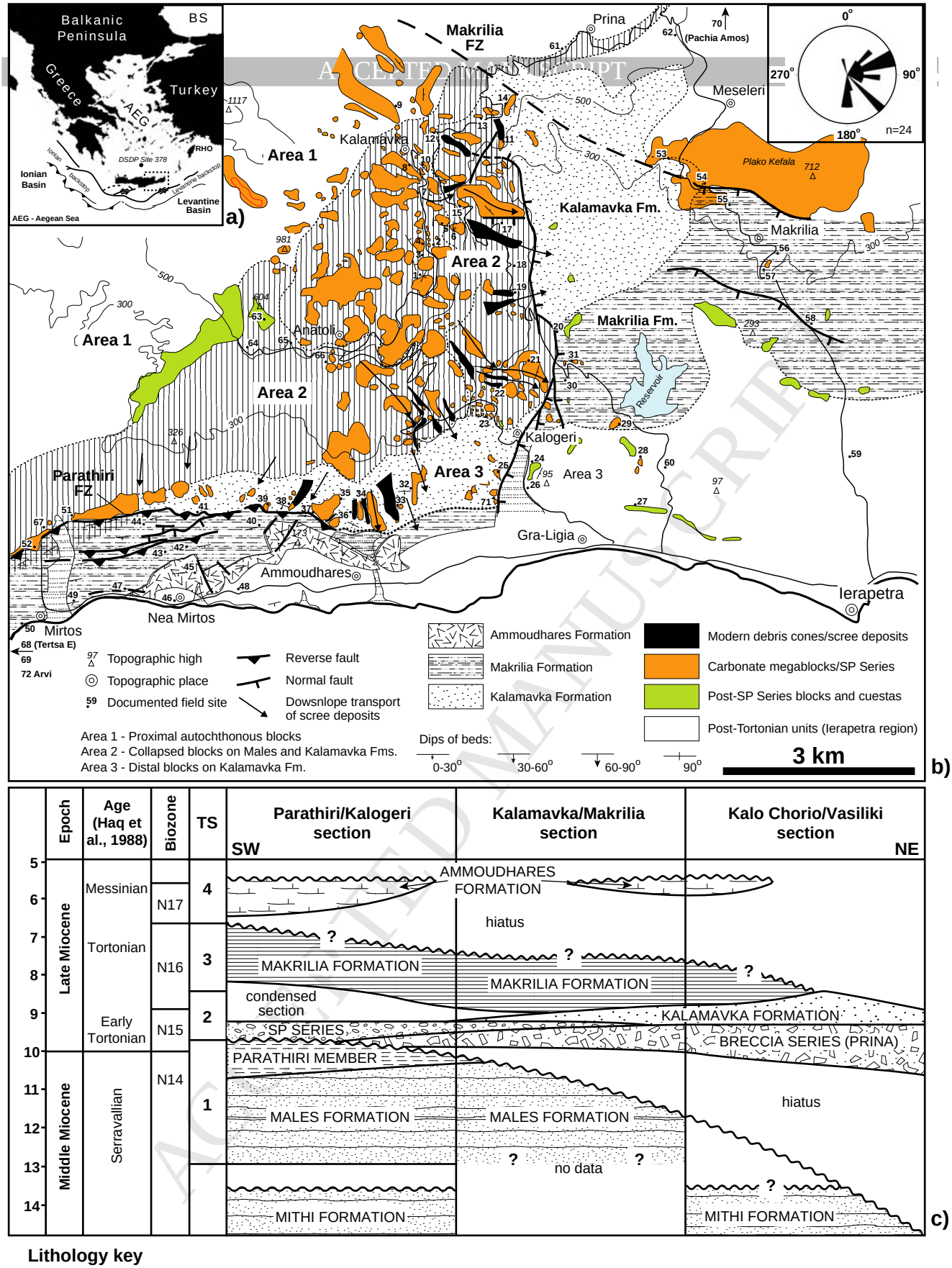
Balkanic Peninsula
BS
Greece
Turkey
AEG
RHO
DSDP Site 378
Ionian Basin
Levantine Basin
AEG - Aegean Sea
a)
Makrilia FZ
Prina
(Pachia Amos)
Meseleri
Kalamavka
Area 1
Area 2
Area 3
Kalamavka Fm.
Plako Kefala
Makrilia
Makrilia Fm.
Reservoir
Anatoli
Kalogeri
Parathiri FZ
Gra-Ligia
Ammoudhares
Ierapetra
Nea Mirtos
Mirtos
68 (Tertsa E)
72 Arvi
Topographic high
Topographic place
Documented field site
Reverse fault
Normal fault
Dowsnlope transport of scree deposits
Area 1 - Proximal autochthonous blocks
Area 2 - Collapsed blocks on Males and Kalamavka Fms.
Area 3 - Distal blocks on Kalamavka Fm.
Ammoudhares Formation
Makrilia Formation
Kalamavka Formation
Modern debris cones/scree deposits
Carbonate megablocks/SP Series
Post-SP Series blocks and cuestas
Post-Tortonian units (Ierapetra region)
Dips of beds:
0-30°
30-60°
60-90°
90°
3 km
b)
n=24
Epoch
Age (Haq et al., 1988)
Biozone
TS
Parathiri/Kalogeri section
Kalamavka/Makrilia section
Kalo Chorio/Vasiliki section
SW
NE
Late Miocene
Middle Miocene
Messinian
Tortonian
Early Tortonian
Serravallian
N17
N16
N15
N14
AMMOUDHARES FORMATION
hiatus
MAKRILIA FORMATION
condensed section
SP SERIES
KALAMAVKA FORMATION
BRECCIA SERIES (PRINA)
PARATHIRI MEMBER
MALES FORMATION
no data
MITHI FORMATION
c)
Lithology key
Bioclastic sands and chalks
Chalk and bioclastic sands
Marine fan-delta sandstones and sands
Deep-marine shales and sands
Fluvio/deltaic continental siliciclastics
Stratified boulder conglomerates
Limestone breccia
TS - Tectonic sequences sensu ten Veen and Postma (1999)

Figure 3 -

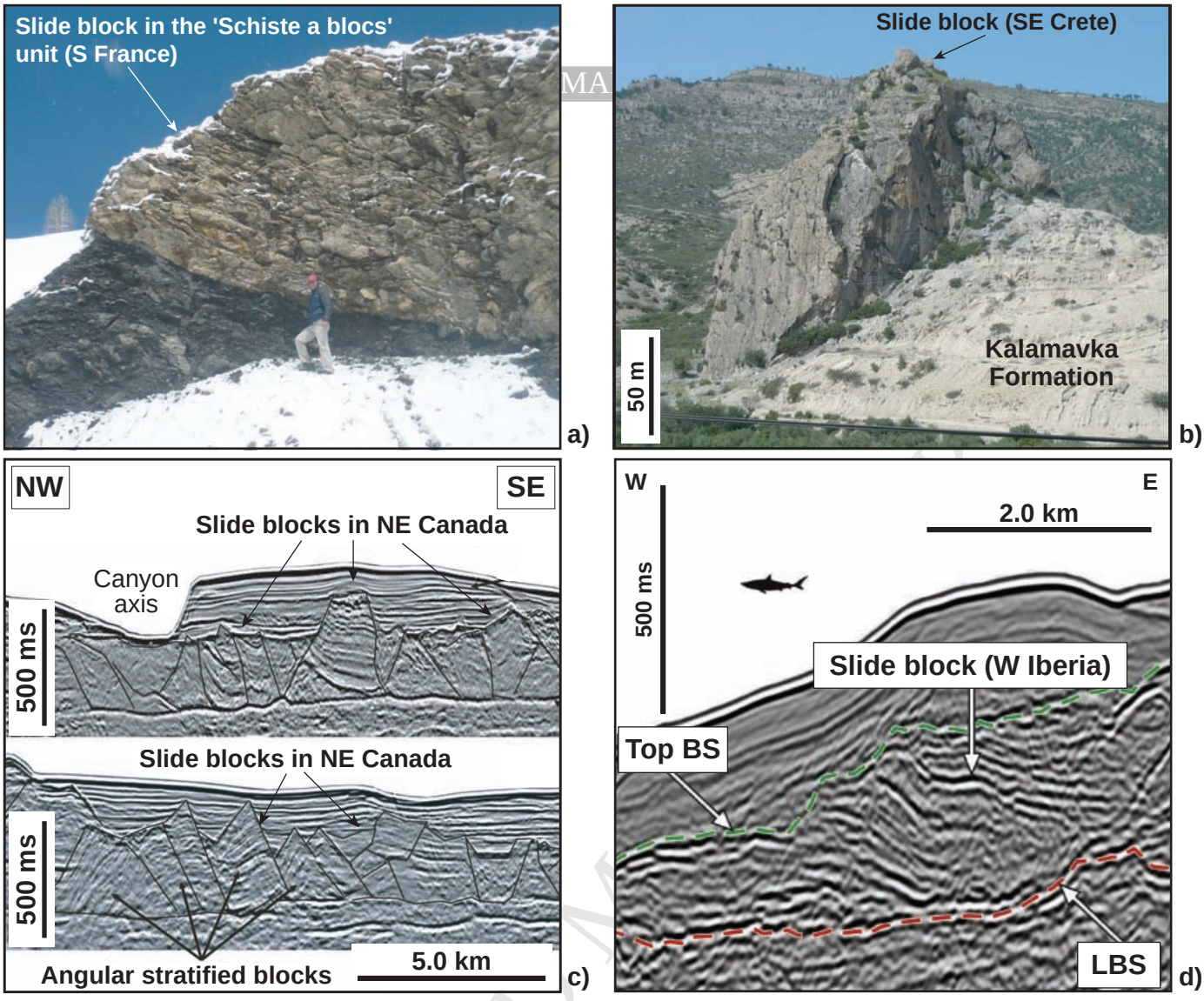

Figure 4 -

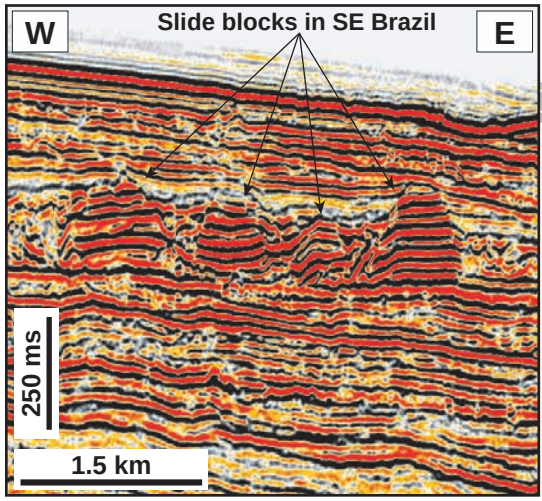

a)

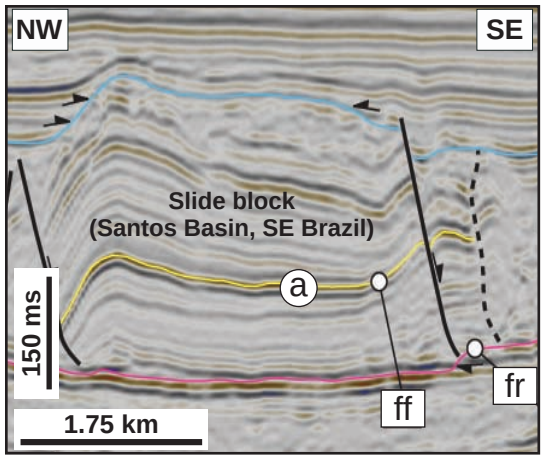

b)

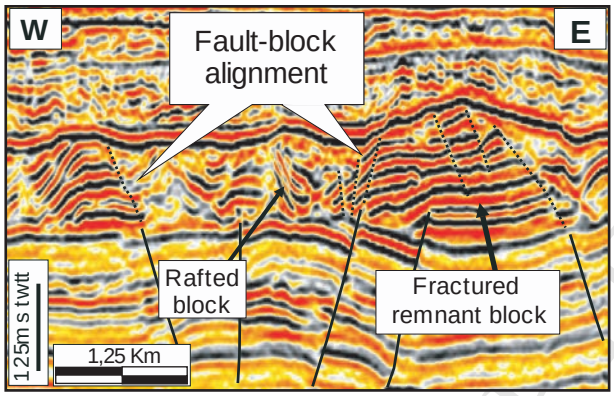

c)

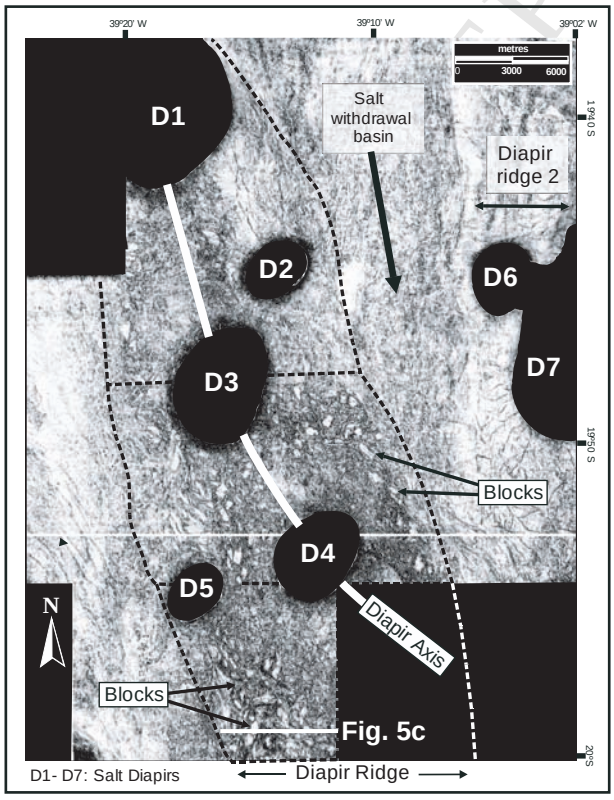

d)

Figure 5 -

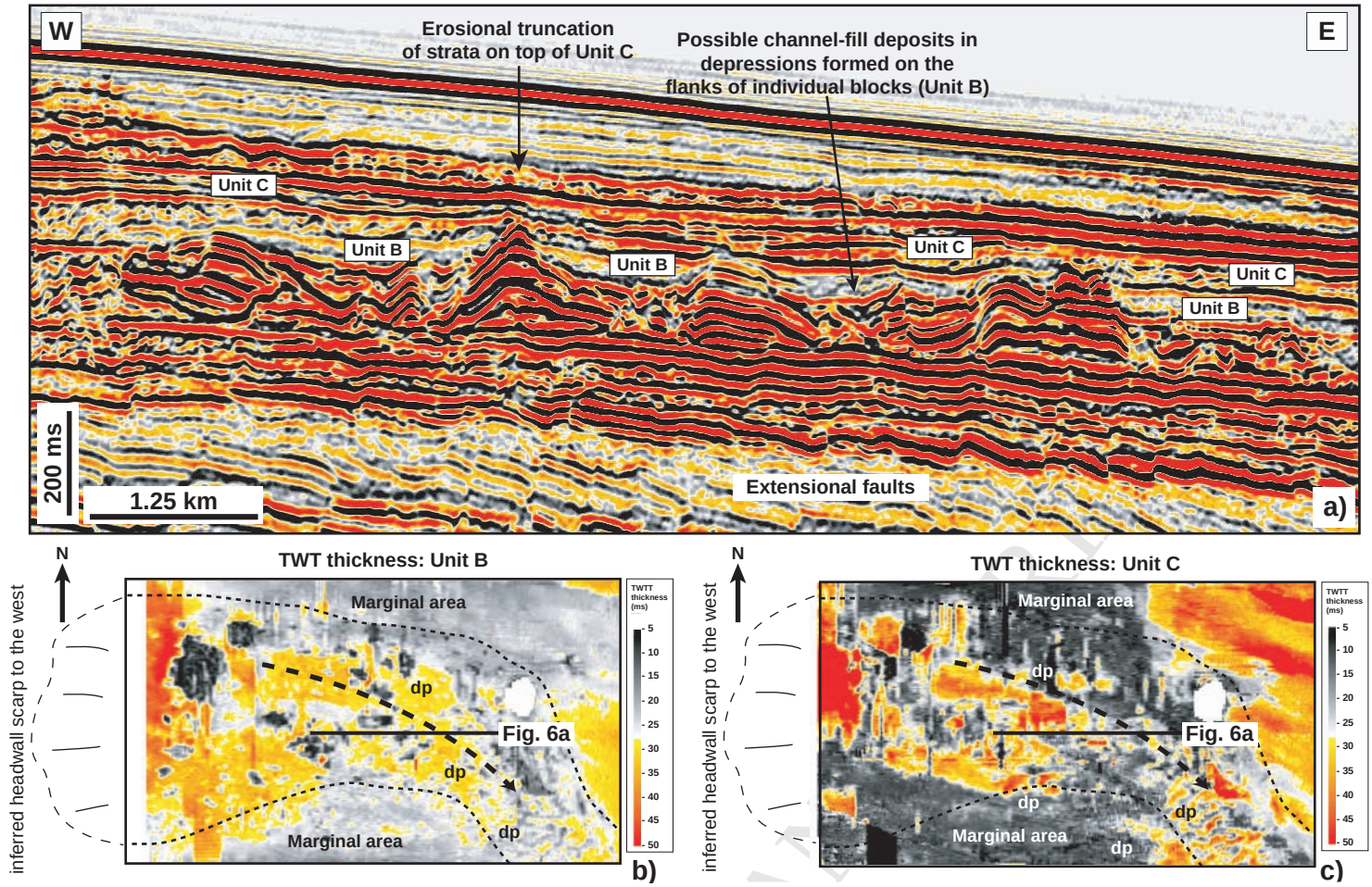

Figure 6 -

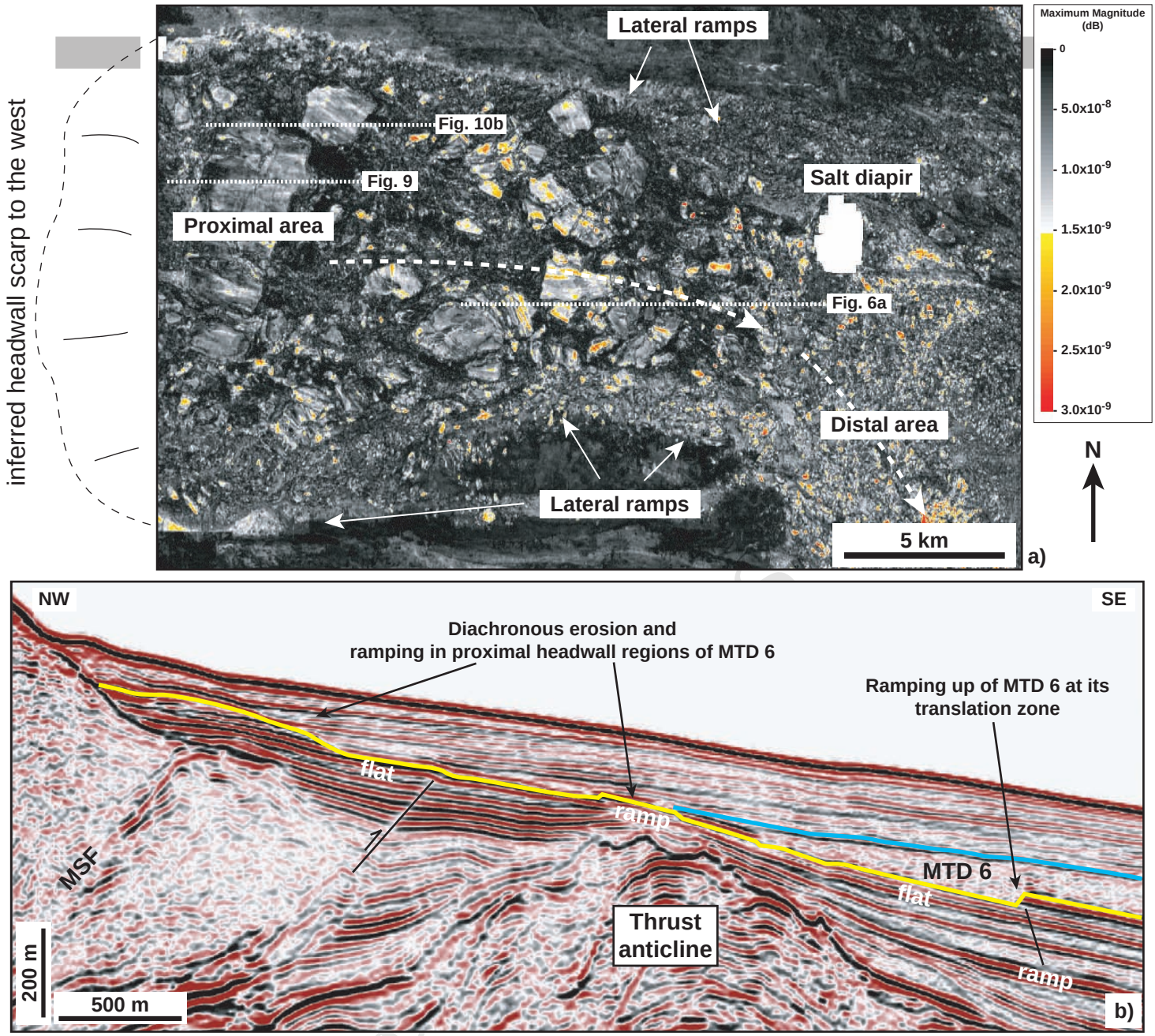
inferred headwall scarp to the west
Lateral ramps
Fig. 10b
Fig. 9
Proximal area
Salt diapir
Fig. 6a
Distal area
Lateral ramps
5 km
a)
Maximum Magnitude (dB)
0
5.0x10-8
1.0x10-9
1.5x10-9
2.0x10-9
2.5x10-9
3.0x10-9
N
NW
SE
Diachronous erosion and ramping in proximal headwall regions of MTD 6
Ramping up of MTD 6 at its translation zone
flat
ramp
MSF
MTD 6
flat
Thrust anticline
ramp
200 m
500 m
b)
MTD 6 thickness on basal shear zone structural map
Thickness (m)
200
160
120
80
40
0
C0001
C0004
C0008A
C0008C
C0010
C0018A
A1
A2
A3
A4
A5
ramp
Fig.7b
Figure
MTD 6
N
3 km
A1 to A5 - Thrust anticlines
c)

Figure 7 -

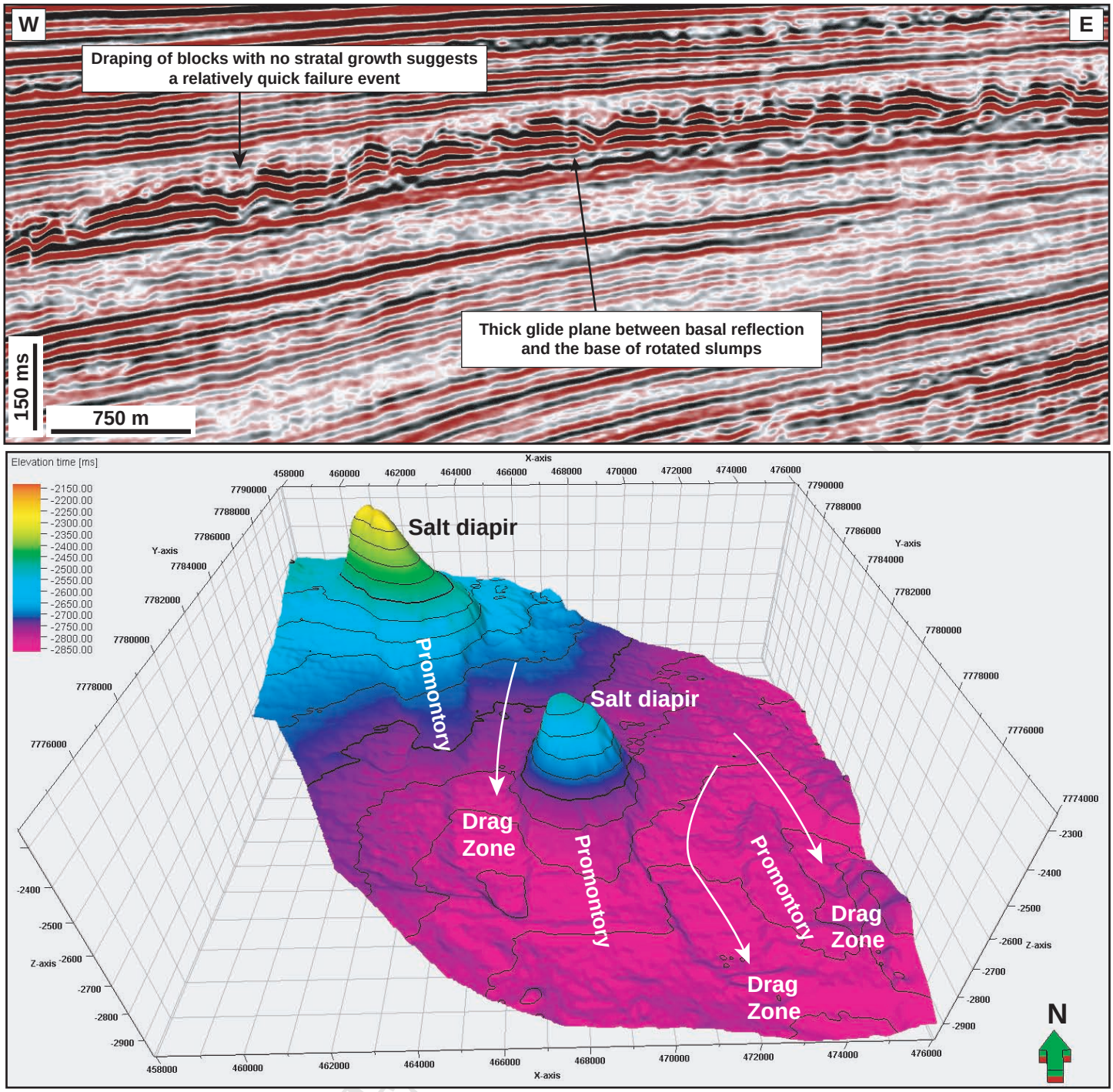

Figure 8 -

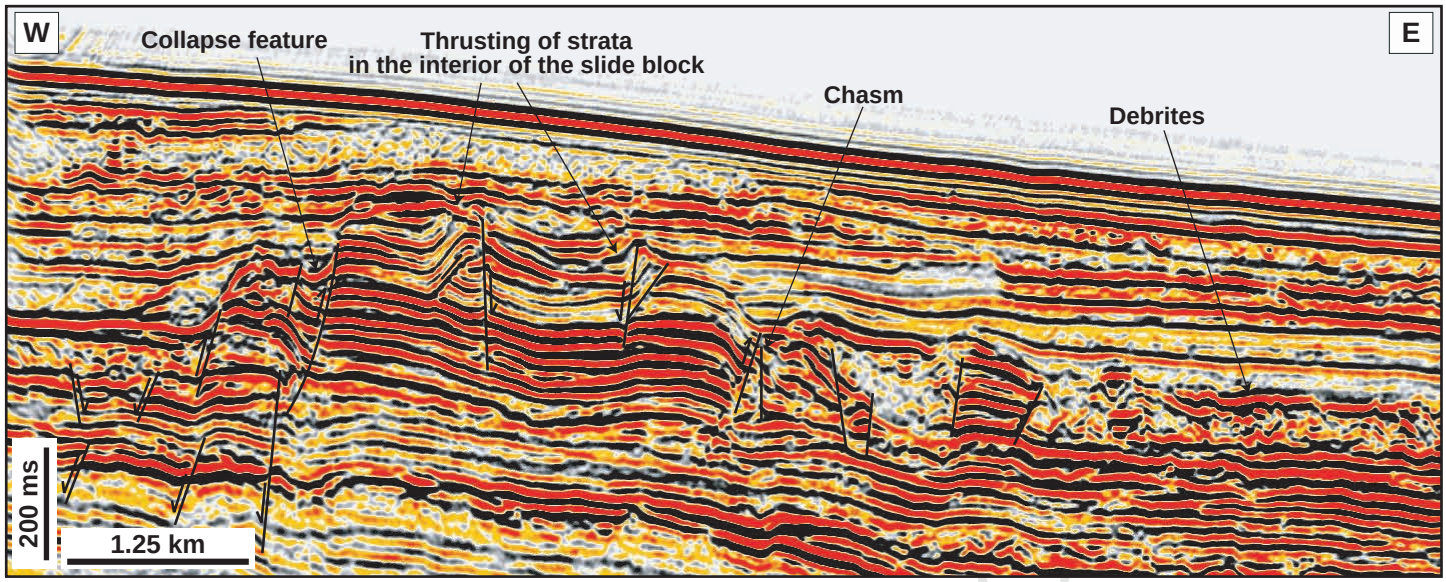

Figure 9 -

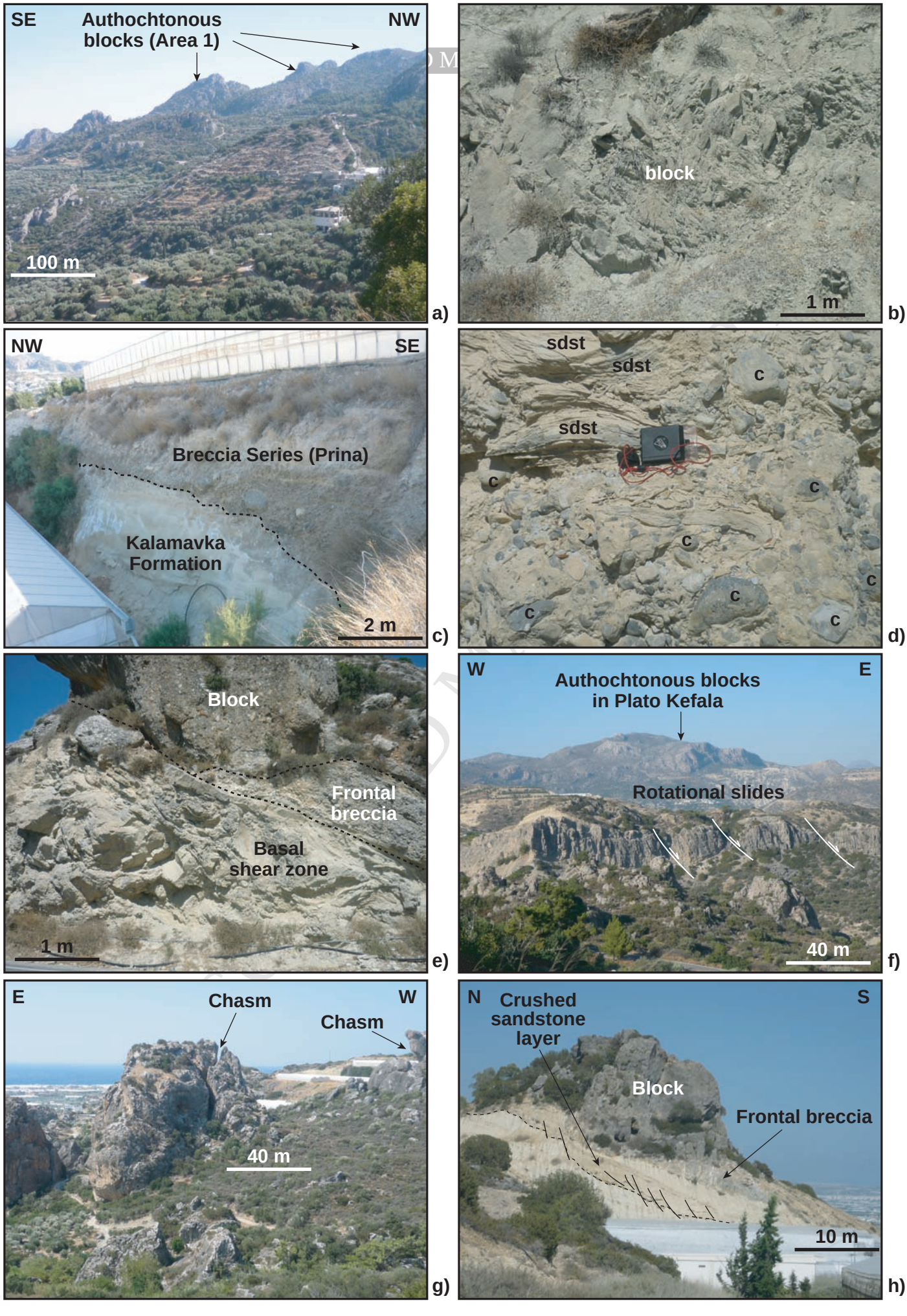
SE
Authochtonous blocks (Area 1)
NW
100 m
a)
block
1 m
b)
NW
SE
Breccia Series (Prina)
Kalamavka Formation
2 m
c)
sdst
sdst
sdst
c
d)
Block
Frontal breccia
Basal shear zone
1 m
e)
W
E
Authochtonous blocks in Plato Kefala
Rotational slides
40 m
f)
E
W
Chasm
Chasm
40 m
g)
N
S
Crushed sandstone layer
Block
Frontal breccia
10 m
h)

Figure 10 -

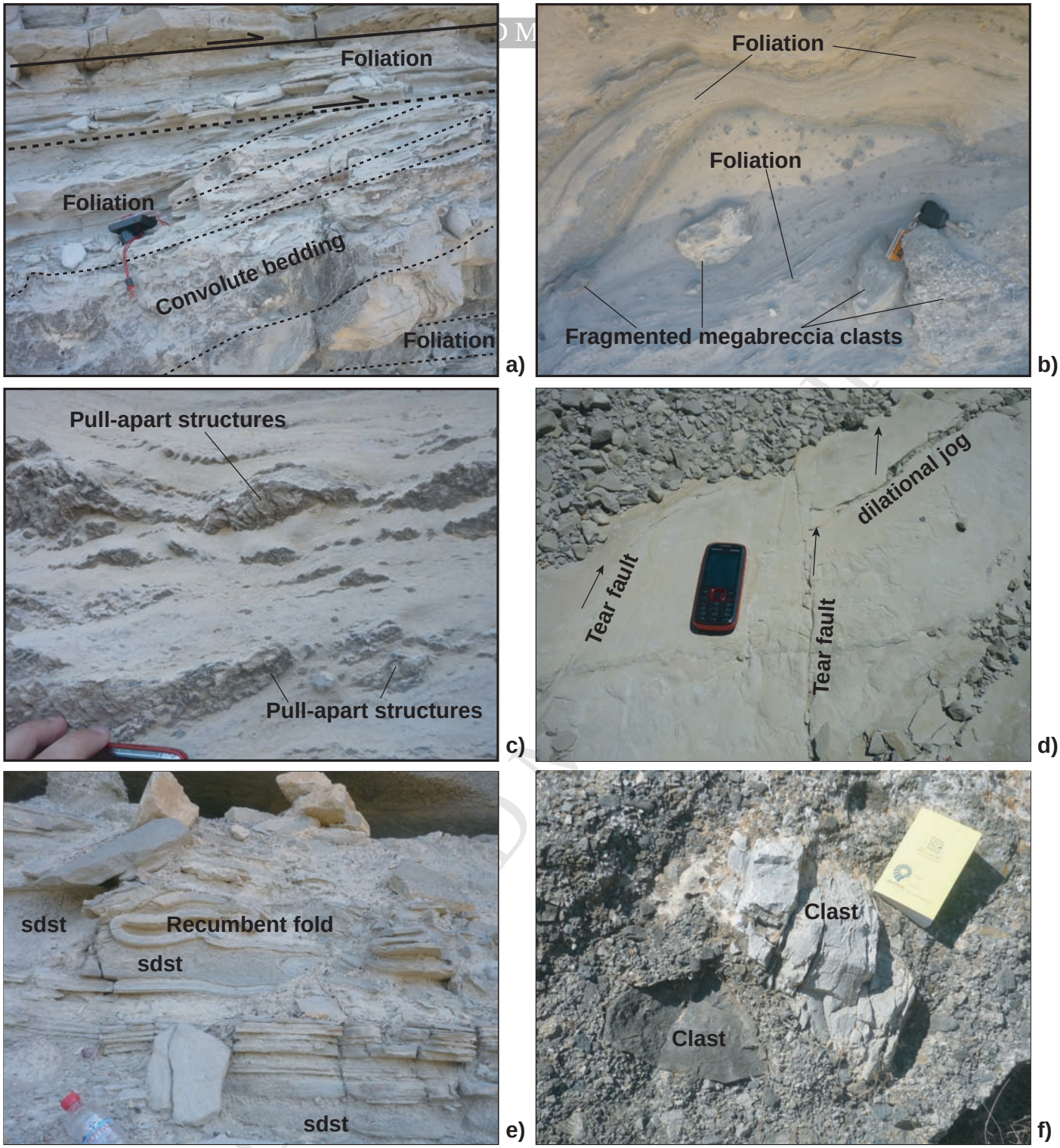
Foliation
Foliation
Convolute bedding
Foliation
a)
Foliation
Foliation
Fragmented megabreccia clasts
b)
Pull-apart structures
Pull-apart structures
c)
dilational jog
Tear fault
Tear fault
d)
sdst
Recumbent fold
sdst
sdst
e)
Clast
Clast
f)

Figure 11 -

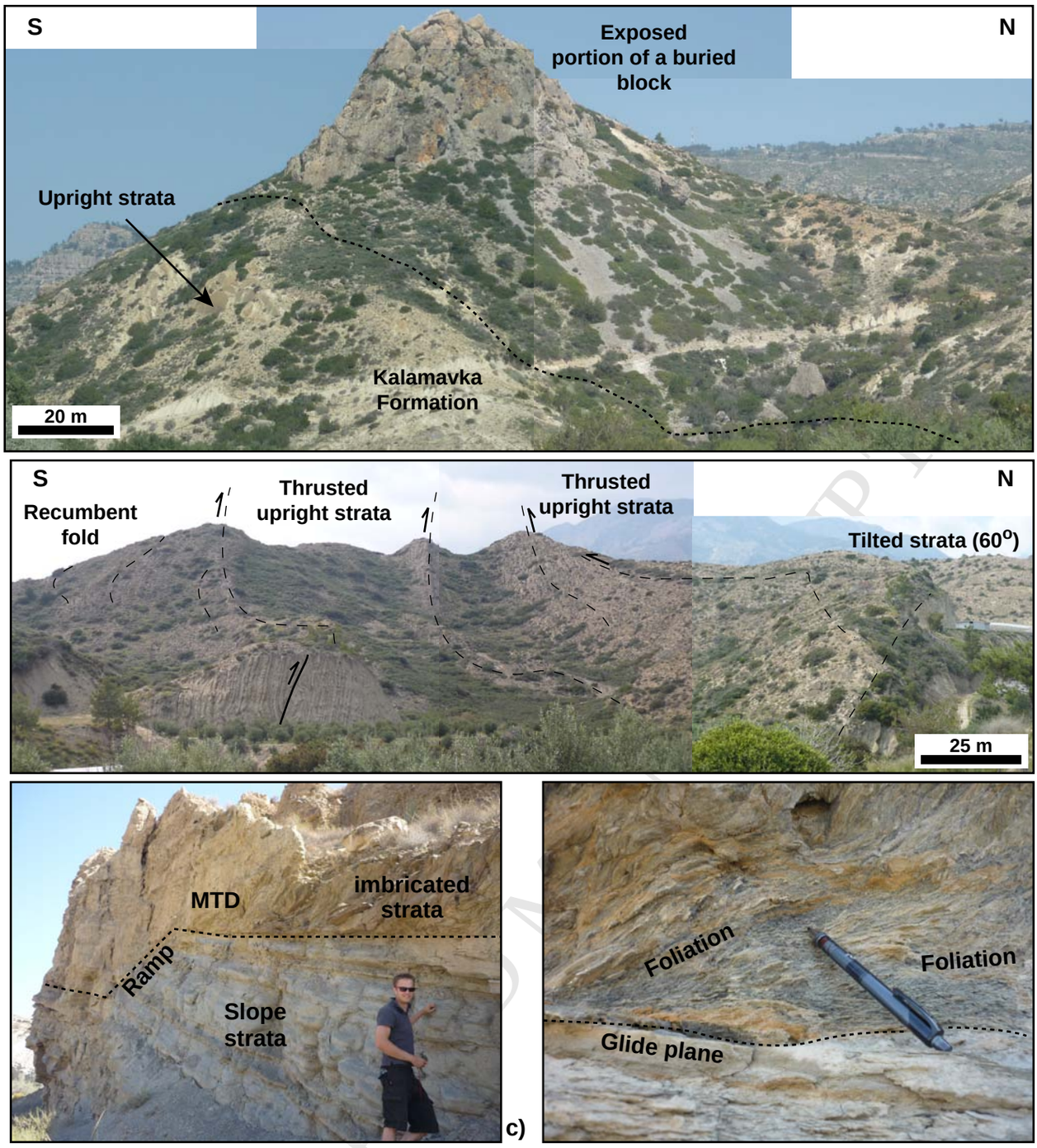

Figure 12 -

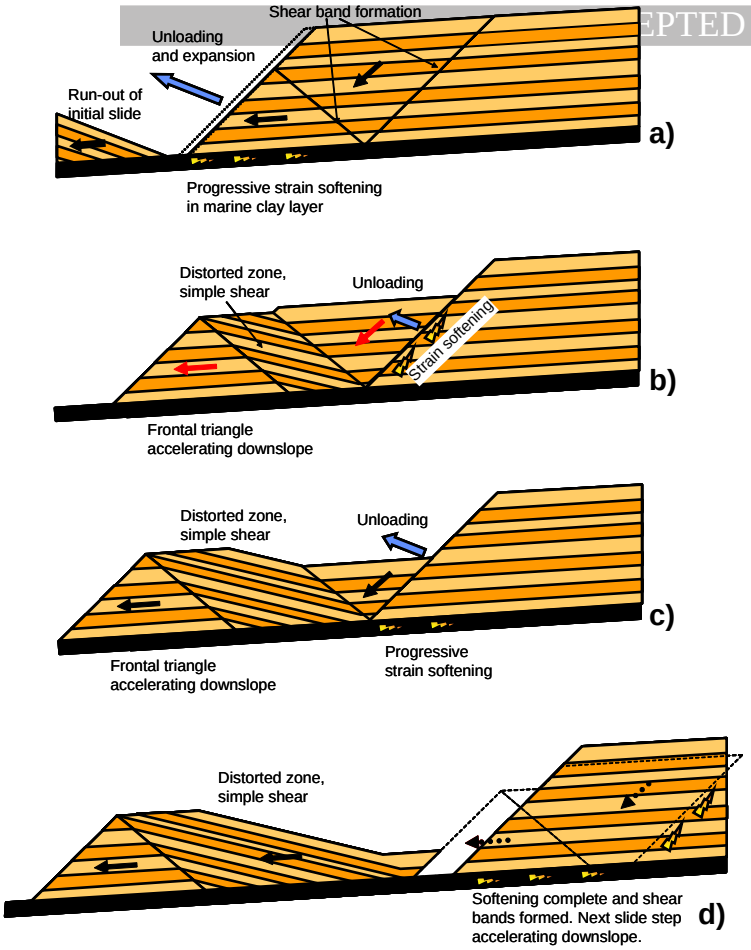

Figure 13 -

Figure 14

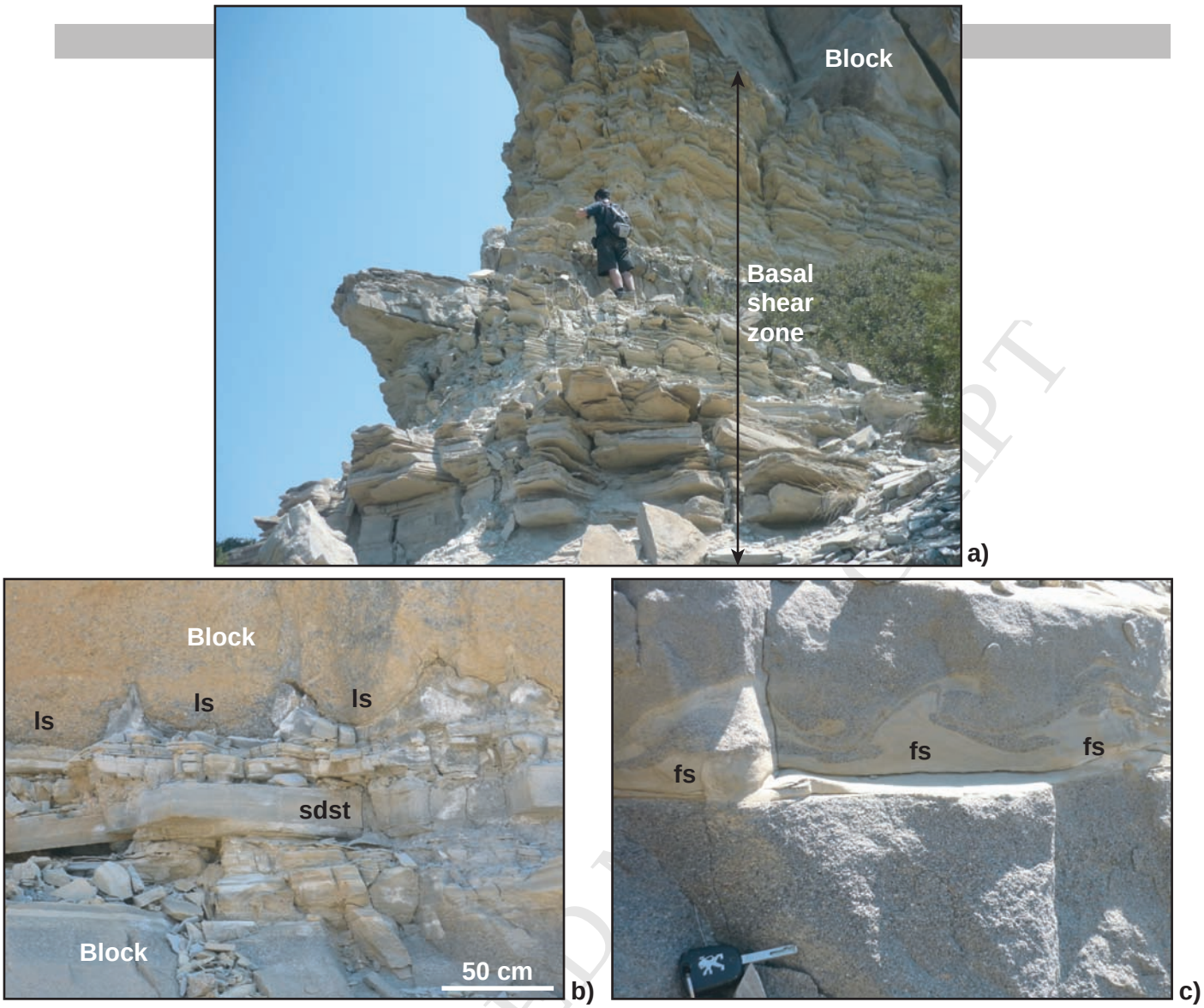

Figure 14 -

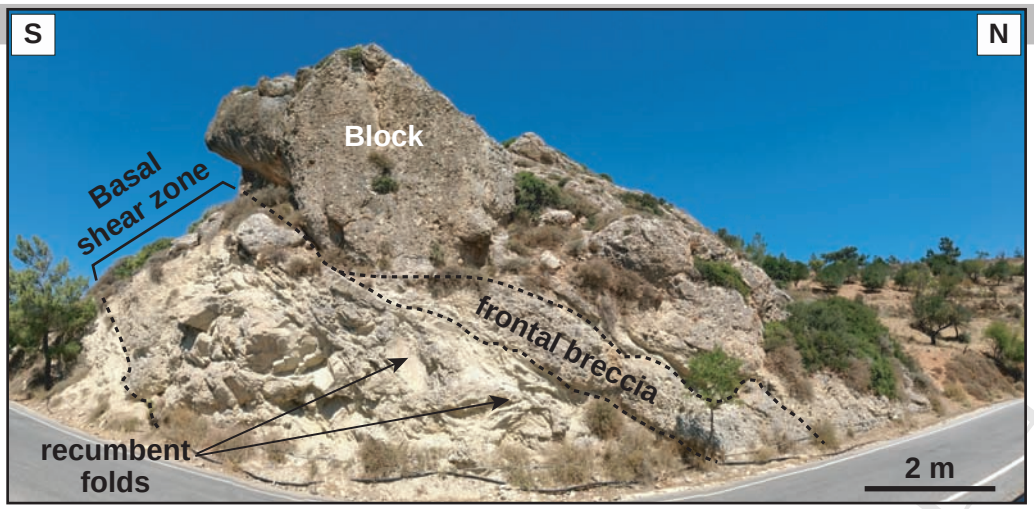

a)

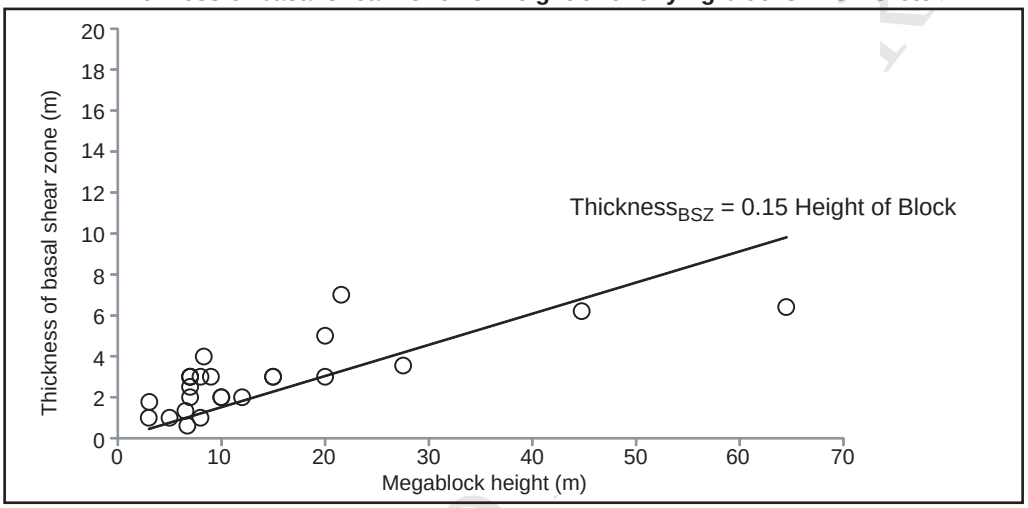

b)

Figure 15 -

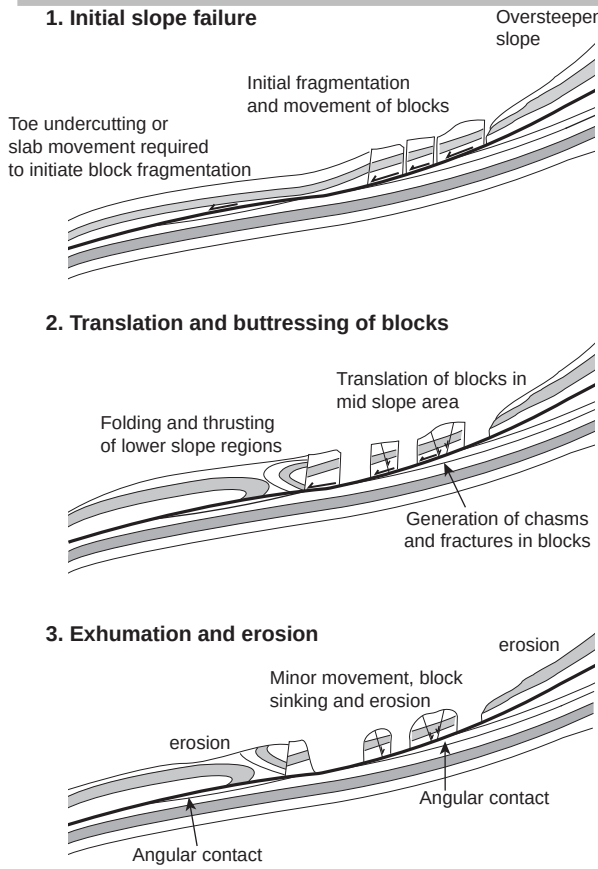

Figure 16

Figure 17

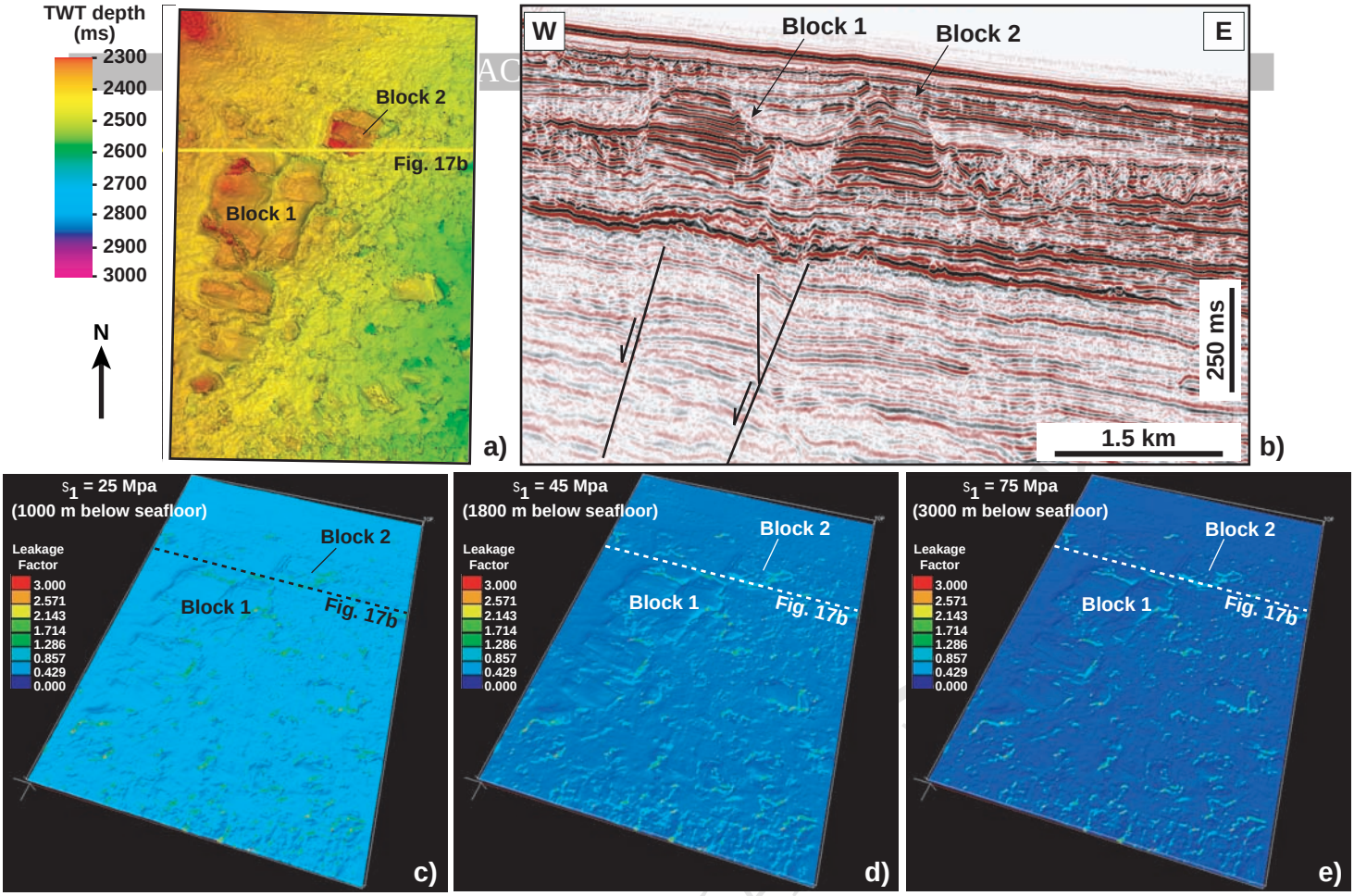

Figure 17 -

Submarine slide blocks are associated with major instability events;

They focus fluid flow to generate reservoirs for hydrocarbons and mineralization;

Meso- and microstructures reflect shearing within and below megablocks;

Blocks mark the sudden release of overburden pressure in deep-water basins.